European Journal of Agronomy 178 (2026) 128152

Contents lists available at ScienceDirect

European Journal of Agronomy

journal homepage: www.elsevier.com/locate/eja

Water-saving and economic benefits of a soil moisture threshold-based irrigation strategy for cotton in Xinjiang under climate change

Bin Chen [a,1], Linjia Yao [b,1], Yadong Liu [c], Mohamed Amine Benaly [d], Changqing Yan [e], Genghong Wu [a,*], Ronghao Guan [f,g], Yi Li [f], Dongyan Zhang [h], Jie Bai [i], Qiuxiang Tang [j], Jianqiang He [f], Hao Feng [a], Qiang Yu [a], Gang Zhao [a,*]

[a] State Key Laboratory of Soil and Water Conservation and Desertification Control, College of Soil and Water Conservation Science and Engineering, Northwest A&F University, Yangling, Shaanxi 712100, China
[b] College of Natural Resources and Environment, Northwest A&F University, Yangling, Shaanxi 712100, China
[c] Shaanxi Meteorological Service Center of Agricultural Remote Sensing and Economic Crops, Xi'an 710016, China
[d] International Waterd Research Institute, Mohammed VI Polytechnic University (UM6P), Benguerir 43150, Morocco
[e] College of Intelligent Equipment, Shandong University of Science and Technology, Taian 271019, China
[f] Key Laboratory for Agricultural Soil and Water Engineering in Arid Area of Ministry of Education, Northwest A&F University, Yangling 712100, China
[g] Yellow River Institute of Hydraulic Research, Yellow River Conservancy Commission, Zhengzhou, Henan 450003, China
[h] College of Mechanical and Electronic Engineering, Northwest A&F University, Yangling, Shaanxi 712100, China
[i] State Key Laboratory of Ecological Safety and Sustainable Development in Arid Lands, Xinjiang Institute of Ecology and Geography, Chinese Academy of Sciences, Urumqi 830011, China
[j] College of Agronomy, Xinjiang Agricultural University, Urumqi 830052, China

ARTICLE INFO

Keywords:
Cotton
Soil moisture threshold-based irrigation
AquaCrop
Economic benefits
Climate change

ABSTRACT

Climate change and growing water scarcity pose major challenges for cotton irrigation in Xinjiang. A soil moisture threshold-based irrigation strategy (SMTIS) offers a promising pathway to improve water-use efficiency and enhance climate resilience. However, regionally optimized, stage-specific soil moisture thresholds that account for crop physiological responses, spatial heterogeneity, and associated economic implications remain poorly quantified. In this study, we coupled the AquaCrop model with a constraint-based nonlinear optimization framework to optimize stage-specific soil moisture thresholds by maximizing irrigation water productivity under a yield loss constraint (≤10%), and evaluate irrigation water requirements and yield responses across Xinjiang for the historical period (2000–2022) and two future periods (2031–2050 and 2061–2080). Validation of the AquaCrop model against canopy cover, aboveground biomass, and seed cotton yield achieved high accuracy (R^2 = 0.80–0.95; index of agreement = 0.96–0.99). Compared with conventional irrigation strategy, SMTIS reduced seasonal irrigation amounts by an average of approximately 247 mm across all periods. Irrigation water productivity increased by an average of 0.83 kg m^{-3}, with peak gains approaching 1.0 kg m^{-3} under high-emission scenarios in the 2070 s. During the historical period, SMTIS generated a mean economic benefit of 1.27×10^3 CNY ha^{-1} across all regions. Regression analysis revealed that climatic factors (particularly reference evapotranspiration and precipitation) dominated SMTIS effectiveness, while soil properties played a secondary but increasingly important role under future climate conditions. Overall, SMTIS emerged as a robust and climate-resilient irrigation strategy that enables substantial irrigation water savings and supports effective irrigation planning and water management in arid cotton-growing regions.

1. Introduction

Climate change is introducing increasing uncertainty into global agricultural systems, particularly in arid and semi-arid regions where limited water availability is the primary constraint on productivity (Mao et al., 2025). Xinjiang, located in northwestern China, supplies over 90%

* Corresponding authors.
E-mail addresses: wugh@nwafu.edu.cn (G. Wu), gang.zhao@nwafu.edu.cn (G. Zhao).
[1] These authors contributed equally to this work.

https://doi.org/10.1016/j.eja.2026.128152
Received 17 October 2025; Received in revised form 26 January 2026; Accepted 2 May 2026
Available online 9 May 2026

of China's cotton but relies heavily on extensive irrigation (Geng et al., 2023; Hu et al., 2021; National Bureau of Statistics of China, 2022) (Fig. S1). Conventinal irrigation practices, typically involving fixed-interval applications that replenish soil moisture to field capacity, have ensured yield stability but at the cost of excessive water consumption, groundwater depletion, soil salinization, and increased environmental pressure (Geng et al., 2023; Guan et al., 2025, 2024; Li et al., 2024a; Song et al., 2023). Moreover, climate projections indicate intensifying water scarcity and increasing hydroclimatic variability in Northwest China (Liu et al., 2024). Under these combined pressures, improving irrigation water productivity (IWP)—defined as the ratio of yield to seasonal irrigation amount—is no longer merely a technical objective, but a critical requirement for sustaining cotton production and farm profitability in the region (Shao et al., 2022). This calls for a transition from conventional fixed-interval irrigation practices toward more robust, water-saving strategies that can maintain yield stability under increasing climate variability.

Soil moisture threshold (SMT)-based irrigation has emerged as a promising scheduling paradigm for improving water use efficiency by aligning irrigation triggering with crop water-stress sensitivity across phenological stages (Liu et al., 2025; Xiao et al., 2023). In practice, defining these SMTs requires a metric that is both physiologically sound and transferable. While thresholds based on field capacity (FC) or soil matric potential are common, they are either site-specific or require dense instrumentation, restricting their regional scalability (He et al., 2020; Liu et al., 2025; Pan et al., 2019; Xiao et al., 2023). In contrast, thresholds based on total available water (TAW) depletion offer a distinct advantage: by normalizing soil water availability between FC and permanent wilting point, TAW-based criteria are universally transferable across diverse soil types (Kelly and Foster, 2021; Madramootoo and Mortel, 2025). However, a critical knowledge gap remains: how to determine the optimal combination of thresholds for different growth stages? Since cotton sensitivity to irrigation varies dynamically throughout the season (Ma and Li, 2002), finding the ideal threshold configuration that balances yield stability and water savings under climate uncertainty is a complex non-linear optimization problem (Liu et al., 2025; Moghbel and Aguilar, 2025). Traditional field experiments are prohibitively costly and time-constrained to exhaustively explore this combinatorial space or to evaluate the robustness of candidate strategies under future decadal climate variability and extreme events. This limitation underscores the necessity of a modeling-based optimization framework for designing robust stage-specific SMT irrigation strategies.

Process-based crop models provide an effective complement to field trials by integrating physiological processes, soil water balance, and yield responses under diverse conditions (García-Vila and Fereres, 2012; Rötter et al., 2018; Zhou et al., 2025). Compared with traditional experiments, such models enable the systematic evaluation of irrigation thresholds across extensive spatial and temporal scales (Himanshu et al., 2019; Thorp, 2020). Among existing crop models, AquaCrop stands out for maintaining an optimal balance between robustness and simplicity (Kelly and Foster, 2021; Zhang et al., 2025). Unlike more physiologically detailed models, AquaCrop requires substantially fewer input parameters, which reduces calibration uncertainty in data-scarce regions while achieving high simulation accuracy under water-limited conditions (Raes et al., 2009). The model has been extensively validated for cotton under full, deficit, and regulated irrigation regimes, demonstrating reliable performance in reproducing canopy development, biomass accumulation, and yield responses to soil moisture constraints (Jiang et al., 2025; Li et al., 2024b; Tan et al., 2018). Given its parameter parsimony and demonstrated applicability in Xinjiang, AquaCrop provides an well-suited platform for optimizing irrigation strategies under changing climatic conditions.

Although AquaCrop has been frequently applied to evaluate and optimize irrigation strategies (Du et al., 2024; Linker et al., 2016; Zhang et al., 2022; Zhu et al., 2024), most existing studies still rely on a limited set of predefined scenario simulations (i.e., trial-and-error approaches) rather than formal mathematical optimization frameworks. As a result, they are unable to reliably identify globally optimal solutions for irrigation scheduling problems characterized by complex, non-linear crop–soil–atmosphere interactions. While some recent efforts have coupled crop models with heuristic optimization algorithms (e.g., genetic algorithms) to refine irrigation schedules (Liu et al., 2025; Wang et al., 2025), several critical gaps remain. First, most optimization studies are confined to historical climate conditions, leaving the robustness of optimized irrigation strategies under future high-emission scenarios and intensified warming largely unquantified. Second, existing applications are predominantly conducted at single experimental sites, thereby neglecting the pronounced spatial heterogeneity in soil properties that critically governs SMT behavior across large irrigated regions such as Xinjiang. Third, optimization objectives commonly emphasize either yield maximization or irrigation water reduction, with limited consideration of economic trade-offs that ultimately shape farmer decision-making. Consequently, there is a lack of systematically optimized, stage-specific SMT thresholds that are robust across both spatial heterogeneity and future climate trajectories.

To bridge these gaps, this study couples AquaCrop with a nonlinear optimization framework to derive robust, stage-specific soil moisture threshold–based irrigation strategies (SMTIS) across Xinjiang under both historical and future climate scenarios. Unlike conventional optimization approaches that primarily seek to maximize absolute yield or IWP, our framework identifies threshold configurations that maximize IWP while explicitly constraining yield failure risk (yield loss $< 10\%$) under multidecadal climate variability. Specifically, this study aims to: (1) derive climate-resilient, stage-specific SMTs across Xinjiang's diverse cotton-producing regions using a computationally efficient optimization framework; (2) quantify the associated water savings and IWP gains under both historical (2000–2022) and future (2031–2050 and 2061–2080) climate conditions, and evaluate the economic benefits of these strategies relative to conventional irrigation practices under historical baseline conditions; and (3) elucidate the climatic and edaphic drivers governing the spatial variability in SMTIS performance. By achieving these objectives, this study provides a regional-scale, forward-looking biophysical assessment and delivers actionable irrigation strategies to support sustainable cotton production under a changing climate.

2. Materials and methods

2.1. Study area

The Xinjiang Uyghur Autonomous Region, located in northwestern China (73°40′–96°18′E, 34°25′–48°10′N), covers an area of approximately 1.66×10^6 km^2 (Fig. 1a). The region is divided by the Tianshan Mountains into Northern Xinjiang (NXJ) and Southern Xinjiang (SXJ) (Fig. 1), which exhibit markedly different climatic conditions. NXJ, situated at higher latitudes, is generally cooler and wetter. In contrast, SXJ, shaped by the arid continental climate of the Tarim Basin, is characterized by hotter and drier conditions and substantially stronger evaporative demand (Zhou et al., 2025). These climatic contrasts fundamentally shape regional water availability and determine irrigation requirements. This study includes 10 experimental sites distributed across both subregions (Fig. 1b), with detailed meteorological characteristics provided in Table S1. Climatic conditions during the cotton growing season (April to October) are illustrated in Fig. 1c–f. Mean temperatures range from 15 to 25 °C (Fig. 1c), with higher values observed in the Tarim Basin and Turpan region. Precipitation remains low throughout the area (Fig. 1d), with most locations receiving less than 200 mm. Reference evapotranspiration (ET_0) is relatively high (500–1300 mm; Fig. 1e). Additionally, the region accumulates considerable growing degree days (GDD), up to 2500 °C·day (Fig. 1f), which are favorable for the growth and development of heat-loving cash crops

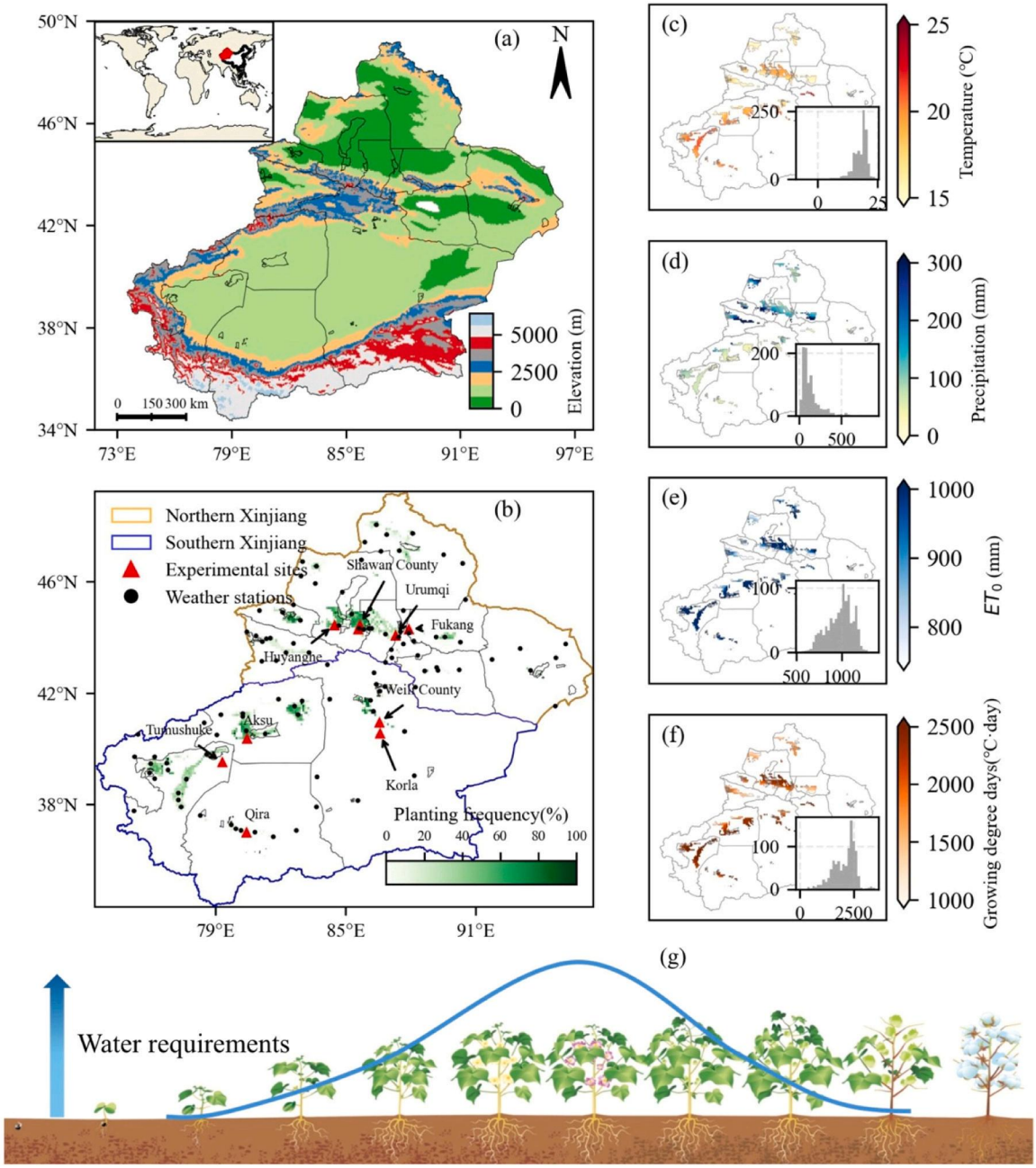

Fig. 1. Geographic distribution of cotton cultivation areas and climatic conditions in Xinjiang. (a) Topography and geographic location of Xinjiang. (b) Distribution and regional divisions of cotton planting areas. (c-f) Annual mean temperature, precipitation, reference evapotranspiration (ET_0), and growing degree days (≥10°C) during the cotton growing season (April–October). Spatial meteorological data are derived from ERA5 and represent average conditions from 2000 to 2022. (g) Seasonal dynamics of cotton water requirements across growth stages, showing peak demand and intensity during the flowering and boll-forming stage (>50% of total seasonal water use), followed by the budding stage, with comparatively lower water demand during emergence and boll-opening stages.

such as cotton. Taken together, low precipitation and high evaporative demand make irrigation indispensable for stable cotton production in Xinjiang.

Beyond ensuring adequate water supply, further gains in water-use efficiency depend on aligning irrigation with crop physiological demand. In particular, leveraging phenology-driven differences in water requirements provides a practical lever to optimize allocation under water-limited conditions (Fig. 1g). Water demand is lowest during the seedling stage, increases during squaring, and peaks during flowering and boll setting, which typically accounts for > 50% of seasonal use; demand then declines during boll opening (Ma and Li, 2002). This pronounced intra-seasonal pattern provides a clear rationale for stage-specific, demand-driven irrigation strategies in Xinjiang.

2.2. *The technical route*

The technical route of this study consists of five steps (Fig. 2). First, observed data on cotton yield, growth, weather, soil properties, and management were collected for model calibration and validation. Subsequently, the AquaCrop model was calibrated and validated at 10 experimental sites using parameter sets of 15 widely cultivated cotton varieties, with model performance evaluated against canopy cover, aboveground biomass, and seed cotton yield. In the third step, both conventional irrigation strategy (CIS) and SMTIS were designed. Site-

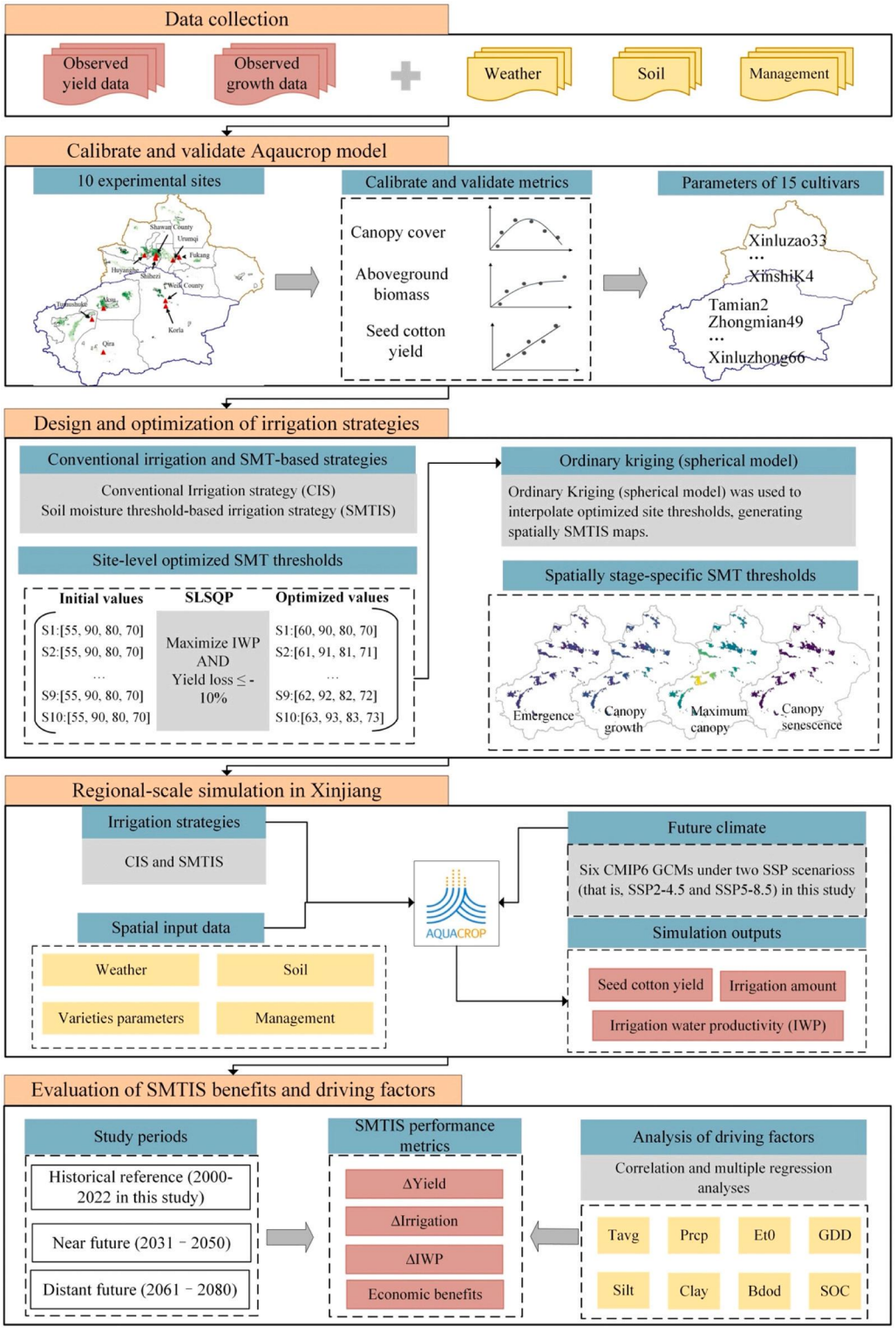

Fig. 2. Schematic overview of the technical framework for developing soil moisture threshold–based irrigation strategies for cotton in Xinjiang using the AquaCrop model. Abbreviations: Xinluzao33, XinshiK4, Zhongmian49, Xinluzhong66, and Tamian2 = representative cotton cultivar parameter sets used for model calibration and validation; CIS = conventional irrigation strategy; SMTIS = soil moisture threshold–based irrigation strategy; SLSQP = Sequential Least Squares Quadratic Programming (optimization algorithm); IWP = irrigation water productivity; ΔYield, ΔIrrigation, and ΔIWP = changes in yield, irrigation, and IWP under SMTIS relative to CIS (SMTIS − CIS); GCMs = general circulation models; SSP = Shared Socioeconomic Pathway (scenarios SSP2-4.5 and SSP5-8.5); Tavg = mean temperature during the cotton growing season; Prcp = precipitation during the growing season; ET_0 = reference evapotranspiration during the growing season; GDD = growing degree days during the growing season; Silt, Clay = soil texture composition (%); Bdod= bulk density; SOC = soil organic carbon.

specific SMTs were optimized using the sequential least squares programming (SLSQP) algorithm to maximize IWP under a yield loss $\leq$ 10% constraint, and spatially SMTs maps were generated through Ordinary Kriging. These optimized thresholds provided the basis for the fourth step, in which AquaCrop was applied to regional-scale simulations under historical (2000–2022) and projected future (2031–2050 and 2061–2080) climate scenarios, driven by six general circulation models (GCMs) and two SSPs (SSP2–4.5 and SSP5–8.5). Finally, the benefits of SMTIS relative to CIS was assessed in terms of changes in cotton yield (ΔYield), irrigation amount (ΔIrrigation), irrigation water productivity (ΔIWP), and economic benefits (EB), while the driving factors—including mean temperature, precipitation, ET_0, soil organic carbon, bulk density, and soil texture—were identified through correlation and regression analyses.

2.3. Data sources and processing

This study integrates multi-source datasets—including field trials, meteorological observations, climate projections, cropland maps, and soil attributes—to support model calibration and regional simulations in Xinjiang. Field observations were compiled from 10 cotton experimental sites spanning diverse agro-environmental conditions (Table 1).

The primary variables included leaf area index (LAI), aboveground biomass, and seed cotton yield; where available, management information (e.g., planting date, irrigation scheduling, and tillage) was also recorded. Specifically, to capture the physiological dynamics across growth stages, LAI data were collected as a continuous time series (typically 4–6 measurements) spanning from seedling to maturity for each site-year. For model simulations, canopy cover (CC) was estimated from LAI using the empirical relationship proposed by García-Vila et al. (2009) :

$$CC = \frac{1 - e^{-\frac{LAI}{1.3}}}{1 + e^{-\frac{LAI}{1.3}}} \quad (1)$$

Among these sites, a two-year field experiment was conducted at the Shihezi in 2021–2022, where LAI, aboveground biomass, and yield of the cultivar Xinluzhong46 were measured. Three additional sites—Aksu, Fukang, and Qira—belong to the Chinese National Ecosystem Research Network (CERN; https://www.cnern.org.cn), which provides long-term standardized agricultural observations across multiple cultivars (2005–2020). Data for the remaining six sites (Weili County, Tumushuke, Korla, Huyanghe, Urumqi, and Shawan County) were extracted from peer-reviewed publications. To ensure robust evaluation, each site dataset was consistently split into calibration and validation years according to the cultivar and observation period.

These harmonized datasets provided the basis for analyzing long-term regional patterns in cotton production and water use. Based on observational data from 10 experimental sites, we analyzed the inter-annual variation in cotton yield, irrigation amount, and IWP under this cultivation system (Fig. 3a–c). From 2005–2021, cotton yield increased from 4.72 t ha^{-1} in 2005–6.21 t ha^{-1} in 2021, with an average of 5.21 t ha^{-1} . Seasonal irrigation amount showed substantial interannual variability, averaging 763.16 mm, while IWP exhibited an overall increasing tendency despite fluctuations, with a mean of 0.84 kg m^{-3} . The shaded areas represent the standard deviation among sites, indicating the spatial variability of the observed indicators.

In addition to the field observations, several gridded datasets were used to provide consistent spatial information on cotton cropland distribution, meteorological conditions, and soil properties (Table 2).

Cotton cropland in Xinjiang was delineated from the SPAM 2020 v2.0 global dataset, which provides 5-arcminute resolution crop distribution maps derived through a cross-entropy downscaling approach. The SPAM dataset is widely used due to its high consistency with official agricultural statistics and its reliable representation of spatial crop patterns (International Food Policy Research Institute (IFPRI), 2024).

For regional simulations, historical daily meteorological data (2000–2022) were derived from the ERA5-Land Daily Aggregated reanalysis product, which provides global land surface variables at 0.1° spatial resolution (Copernicus Climate Change Service, 2019). Future daily climate data (2023–2080) were sourced from the NEX-GDDP-CMIP6 v2.0 archive (Thrasher et al., 2022). This dataset downscales CMIP6 model output to ~0.25° resolution using the bias-correction spatial disaggregation method. This method uses quantile mapping to align each model's cumulative distribution with observations from the Global Meteorological Forcing Dataset over a 1960–2014 reference period, and then reinstates long-term trends. Bias correction and downscaling are applied to variables such as daily maximum and minimum temperature, precipitation, humidity, radiation and wind speed; from these we extracted bias-corrected temperature and precipitation and combined them with scenario-specific CO_2 trajectories for our simulations. Projections were drawn from six CMIP6 models (BCC_CSM2_MR, HadGEM3_GC31_LL, FGOALS-g3, IPSL_CM6A_LR, GFDL_ESM4 and MIROC6, see Table S2) under two socio-economic pathways (SSP2–4.5 and SSP5–8.5), capturing a representative range of climate sensitivities and regional responses (O'Neill et al., 2016). Fig. S2 shows projected changes in mean temperature, precipitation, and atmospheric CO_2. In Xinjiang's cotton-growing regions, temperature is projected to increase steadily, with stronger warming under SSP5–8.5, while precipitation remains relatively stable. Atmospheric CO_2 concentrations are projected to increase from current levels (~410 ppm) to approximately 520 ppm under SSP2–4.5 and

Table 1
Summary of sites, data sources, observed variables, cultivars, and calibration/validation years.

Site	Source	Observations	Cultivar	Calibration year	Validation year
Shihezi	Field experiment (this study)	LAI, Biomass Yield	Xinluzhong46	2021	2022
Aksu	Chinese National Ecosystem Research Network (https://www.cnern.org.cn/)	LAI, Biomass, Yield	Zhongmian49	2007	2008
			Tongnong1	2009	2010
			Tamian2	2012–2014	2015
		LAI, Biomass,	Xinluzhong66	2018	2019
Fukang		Yield	83–1 (local line; exact cultivar name not reported)	2009–2014	2015–2020
			XinshiK4	2005–2006	2007–2008
Qira		LAI, Biomass,	Xinluzao28	2013	2018
		Yield	Yumian15	2015	2016
			Zhongkemian1	2019	2020
Weili County	Meng (2021)	LAI, Yield	Xinluzhong78	2018	2019
Tumushuke	Zhang et al. (2016)	LAI, Yield	Zhongmian49	2014	2015
Korla	Bai et al. (2024)	LAI, Yield	Xinluzhong67	2020	2021
Huyanghe	Kang (2021)	Biomass, Yield	Zhongmiansuo109	2019	2020
Urumqi	Wang et al. (2016)	LAI, Biomass, Yield	Xinluzao26	2010	2011
Shawan	Zhao (2022)	Yield	Xinnongda12	2017	2018

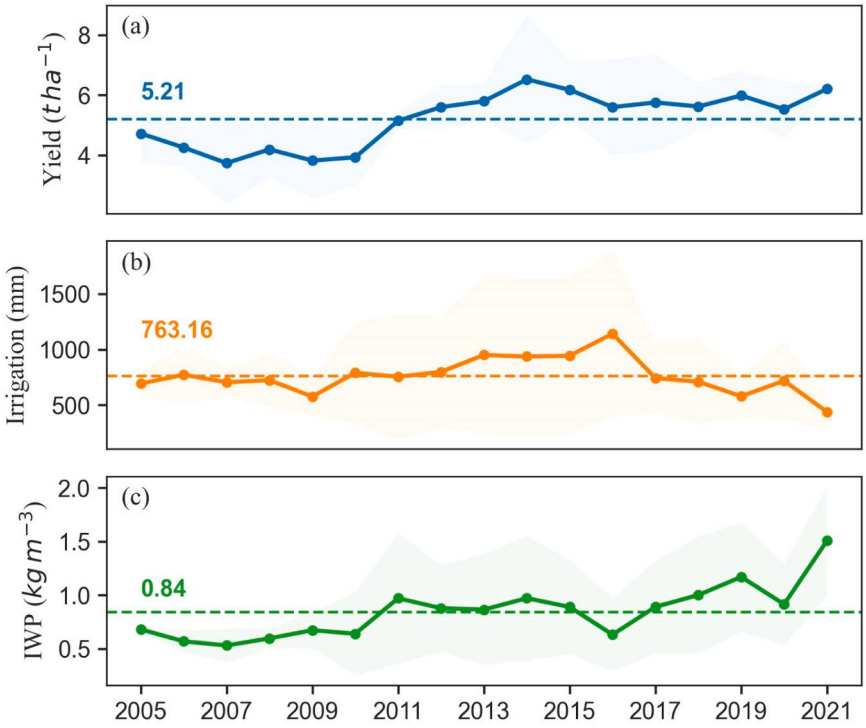

Fig. 3. Long-term trends in seed cotton yield, seasonal irrigation amount, and irrigation water productivity at 10 experimental sites in Xinjiang from 2005 to 2021 (a–c).Temporal trends in average cotton yield (t ha^{-1}), seasonal irrigation amount (mm), and irrigation water productivity (kg m^{-3}) from 2005 to 2021, based on observational data from 10 experimental sites. Solid lines indicate annual means, shaded areas represent the standard deviation among sites, and dashed horizontal lines denote the multi-year averages. Data from 2022 were excluded because only one site-year of observations was available.

Table 2
Spatial datasets with temporal coverage and source links used in this study.

Data name	Data type	Link	Period	Spatial resolution	
				Original	After sampling
SPAM 2020 v2.0	Cropland map	https://doi.org/10.7910/DVN/ZWSFAA	Static	5′	5′(~10 km)
ERA5-Land	Historical meteorological dataset	https://doi:10.24381/cds.68d2bb30	2000–2022	0.1°	
NEX-GDDP-CMIP6	Future meteorological dataset	https://doi:10.5194/hess-16–3309–2012	2031–2080	0.25°	
SoilGrids	Soil dataset	https://doi.org/10.7910/DVN/1PEEY0	Static	5′	

about 650–670 ppm under SSP5–8.5 by the 2070 s.

Soil properties were obtained from a global gridded soil database at 5-arcminute resolution (Poggio et al., 2021). The dataset includes six standard soil layers (0–5 cm, 5–15 cm, 15–30 cm, 30–60 cm, 60–100 cm, and 100–200 cm), and provides key physical and chemical attributes such as soil texture (sand, silt, and clay), bulk density, soil organic carbon, cation exchange capacity, and hydraulic parameters required for crop modeling. All spatial inputs were resampled to 5-arcminute (~10 km) resolution, yielding 1337 cotton cropland simulation grids.

2.4. Model-based simulation of cotton growth and yield

2.4.1. AquaCrop model

The AquaCrop model, developed by the Food and Agriculture Organization, simulates crop growth, biomass accumulation, and yield formation under different water conditions (Todorovic et al., 2009). Designed to balance biophysical realism with parameter simplicity, it captures key soil-plant-atmosphere interactions while remaining robust across diverse climates and management practices. Owing to these features, AquaCrop is widely used for irrigation scheduling, water productivity assessment, and climate impact analysis.

The model consists of four main modules—meteorology, crop, soil, and management—that jointly simulate the soil-plant-atmosphere continuum. Its core mechanism is based on a daily soil water balance and quantifies the effects of water stress on crop productivity. AquaCrop builds on the classical water-yield relationship described in FAO Irrigation and Drainage Paper No. 33 (Doorenbos and Kassam, 1970):

$$\frac{Y_m - Y_a}{Y_m} = K_y\left(\frac{ET_m - ET_a}{ET_m}\right) \tag{2}$$

where Y_m and Y_a are maximum and actual yields, ET_m and ET_a are maximum and actual evapotranspiration. K_y the proportionality factor between relative yield decline and relative reduction in evapotranspiration.

AquaCrop evolves from the K_y approach by separating the actual evapotranspiration (ET) into soil evaporation (E) and crop transpiration (Tr).

$$ET = E + Tr \tag{3}$$

The model assumes that crop yield is primarily driven by transpiration rather than evaporation. Daily crop transpiration is linked to aboveground biomass production (B) via a normalized water productivity parameter (WP^*):

$$B = WP^* \sum_{i=1}^{n} Tr_i \tag{4}$$

where B (kg m^{-2}) is total aboveground biomass, *WP** (kg m^{-2} mm^{-1}) is the normalized water productivity parameter, Tr_i is transpiration (mm) on day i and n is the number of growing days.

The final seed cotton yield (Y, kg m^{-2}) is computed as the products of d aboveground biomass and the harvest index (HI), where HI represents the fraction of total aboveground biomass allocated to the economic yield:

$$Y = HI{\cdot}B \tag{5}$$

2.4.2. Model calibration and validation

In this study, we utilized AquaCrop-OSPy (version 3.0.11), the open-source Python implementation of AquaCrop (Kelly and Foster, 2021). While AquaCrop provides a suite of standard crop parameters for cotton, these parameters necessitate adjustment to align with local environmental and agronomic conditions (Raes et al., 2012). To enhance model reliability for the study region, we calibrated and validated AquaCrop-OSPy using aforementioned field trial data, including canopy cover (CC), aboveground biomass, and seed cotton yield, collected from 10 experimental sites. Prior to calibration, we assumed full pre-planting irrigation across all plots, with initial soil water content set to field capacity. Mulching was applied with a coverage rate of 80% (Tan et al., 2018). Given the deep groundwater table in most parts of Xinjiang, groundwater contribution was excluded from the simulation (Li et al., 2024b).

The calibration process involved iteratively adjusting parameters within the ranges recommended by Raes et al. (2012) and Tan et al. (2018). Calibration and validation were performed independently for each cotton variety at each site, using a trial-and-error approach to fine-tune and correct model parameters based on these reference values. The calibration process began with the simulation of canopy development by adjusting parameters such as maximum canopy cover, the canopy growth coefficient, the canopy decline coefficient, and water-stress parameters. Model outputs were evaluated against observed canopy cover values (Fig. S3 and Fig. S4). Subsequently, aboveground biomass (Fig. S5 and Fig. S6) and seed cotton yield were calibrated. The final calibrated parameters for each cotton variety are provided in Table S3.

2.4.3. Model performance evaluation

We assessed model performance using the coefficient of determination (R^2), root mean square error (RMSE), and the index of agreement (d):

$$R^2 = \left(\frac{\sum_{i=1}^{n} \left(O^i - \overline{O}\right)\left(S^i - \overline{S}\right)}{\sqrt{\sum_{i=1}^{n} \left(O^i - \overline{O}\right)^2 \sum_{i=1}^{n} \left(S^i - \overline{S}\right)^2}} \right) \tag{6}$$

$$\mathrm{RMSE} = \sqrt{\frac{1}{n}\sum_{i=1}^{n} \left(S_i - O_i\right)^2} \tag{7}$$

$$d = \quad 1 - \frac{\sum_{i=1}^{n} \left(S_i - O_i\right)^2}{\sum_{i=1}^{n} \left(|S_i - \overline{O}| + |O_i - \overline{O}|\right)^2} \tag{8}$$

where $O^i$and S^i are observed and simulated values, $\overline{O}$ is the mean of observed values, and n is the sample size. R^2 quantifies the proportion of variance explained; *RMSE* reflects absolute deviations (lower is better); d evaluates overall agreement and is informative when R^2 alone may miss systematic bias. Model performance is generally considered acceptable when $R^2 > 0.5$ or $d > 0.65$; *RMSE* approaching zero indicates high accuracy (Jacovides and Kontoyiannis, 1995; Legates and McCabe, 1999).

2.5. Definition and optimization of irrigation scheduling strategies

2.5.1. Conventional irrigation strategy

In Xinjiang, limited water availability has led to government-regulated rotational irrigation, typically at 5–10 day intervals (Meng, 2021; Wu, 2015). In this study, CIS is represented by a 7-day fixed schedule following Song et al. (2023), with soil moisture replenished to field capacity at each event.

2.5.2. Soil moisture threshold–based irrigation strategy

The SMTIS was implemented in AquaCrop by defining stage-specific soil moisture thresholds as fractions of TAW. Irrigation was automatically triggered once simulated root-zone depletion exceeded the threshold for a given growth stage. The SMTs in four cotton phenological stages were considered: emergence (SMT_1), canopy growth (SMT_2), maximum canopy cover (SMT_3), and senescence (SMT_4) (Liu et al., 2025).

Soil moisture threshold definition

For each experiment site $i = 1, \ldots, 10$ and cotton growth stage $s = 1, \ldots, 4$, the soil moisture threshold is denoted:

$$SMT_{i,s} \in [SMT_{\min}, \quad SMT_{\max}] \tag{9}$$

where $SMT_{i,s}$is the soil moisture threshold (as a fraction of TAW) that triggers irrigation, and $SMT_{\min}$, and $SMT_{\max}$ are the lower and upper bounds of allowable thresholds, set to 55% and 100%, respectively. A lower bound of 55% TAW was imposed to avoid excessive stress during optimization, consistent with FAO-56 guidelines for row crops such as cotton (Allen et al., 1998; Fereres and Soriano, 2007).

Irrigation trigger condition

On day t of year n at site i, the relative root-zone depletion is defined as:

$$D_{i,n,t} = \frac{\theta_{\mathrm{FC},i} - \theta_{i,n,t}}{\theta_{\mathrm{FC},i} - \theta_{\mathrm{PWP},i}}, \quad D_{i,n,t} \in [0,1] \tag{10}$$

where $\theta_{FC,i}$ is the volumetric soil water content at field capacity,

$\theta_{PWP,i}$ is the volumetric soil water content at permanent wilting point, and

$\theta_{i,n,t}$ is the actual soil water content on day t of year n at site i.

Let $s(t)$ denote the growth stage of the crop on day t. Irrigation was triggered when:

$$\mathbb{I}_{i,n,t} = 1 \quad \left\{ D_{i,n,s(t)} \geq SMT_{i,s} \right\} \tag{11}$$

where $\mathbb{I}_{i,n,t}$ represents the irrigation decision variable (1 if irrigation occurs, 0 otherwise) on day t of year n at site i; when triggered, irrigation replenished the soil profile to field capacity.

Optimization framework

The optimization aimed to maximize IWP while constraining yield loss under SMTIS to less than 10% relative to the CIS. This dual-objective design reflects both the regional imperative of improving water-use efficiency and the agronomic requirement of yield stability (Fanuel et al., 2018; Sadati et al., 2014).IWP and yield difference are defined as:

$$\mathrm{IWP} = \quad \frac{Yield}{Irrigation} \tag{12}$$

$$\Delta Yield = \quad Yield_{SMTIS} - Yield_{CIS} \tag{13}$$

where *Yield* is the seed cotton yield (kg ha^{-1}), *Irrigation* is the seasonal irrigation amount (m^3 ha^{-1}), and $\Delta Yield$ is the yield difference between SMTIS and CIS.

For each site, AquaCrop simulations were conducted over the historical period (2000–2022), and annual results for yield and irrigation water were averaged to obtain long-term mean values.

These multi-year averages were then used to calculate irrigation water productivity (see Supplementary Text S1 for the detailed formulation of annual averaging and calculations). The optimization problem for site i is formulated as:

$$\left\{SMT^{*}_{i,1},\ SMT^{*}_{i,2},\ SMT^{*}_{i,3},\ SMT^{*}_{i,4}\right\} = \arg\max_{\{SMT_{i,s}\}_{s=1}^{4}} \overline{IWP}_i\left(\{SMT_{i,s}\}\right) \tag{14}$$

subject to the yield constraint:

$$\frac{\overline{Y}_{\mathrm{CIS},i} - \overline{Y}_i\left(\{SMT_{i,s}\}\right)}{\overline{Y}_{\mathrm{CIS},i}} \le 10\% \tag{15}$$

where $\overline{IWP}_i$ denotes the mean irrigation water productivity, and $\overline{Y}_{\mathrm{CIS},i}$ and $\overline{Y}_i\left(\{SMT_{i,s}\}\right)$ denote the mean yields under CIS and SMTIS, respectively, over the historical period at site i.

These optimized thresholds represent site-specific lower limits for soil moisture that balance the trade-off between maximizing IWP and maintaining yield stability. By integrating local soil hydraulic properties and long-term climate variability, the optimization identifies the critical depletion levels required to minimize non-productive evaporation while ensuring crop water stress remains within a recoverable range (yield loss $\le$ 10%).

The nonlinear constrained optimization problem described above was solved using the Sequential Least Squares Programming (SLSQP) algorithm, a gradient-based iterative method that efficiently handles both equality and inequality constraints (Gong et al., 2023). SLSQP is particularly suitable in this context because irrigation thresholds must remain within physically realistic bounds while simultaneously satisfying yield constraints (Ran et al., 2025). To enhance robustness and reduce sensitivity to initial conditions, each site-level optimization was repeated 1000 times with randomly generated initial threshold values, and the best-performing solution was retained. Detailed descriptions of the optimization configuration—including convergence criteria (e.g., termination tolerance, constraint violation thresholds) and stopping conditions—are provided in Text S2. All optimization runs converged successfully under these criteria, and the stage-specific optimal thresholds for each site are summarized in Table S4.

Because crop water requirements are jointly determined by soil water status and atmospheric demand (Zhang et al., 2021), it is necessary to clarify how atmospheric demand is represented within the modeling framework. In AquaCrop, atmospheric evaporative demand is incorporated through reference evapotranspiration (ET_0), which is calculated using the FAO Penman–Monteith equation (Allen et al., 1998):

$$ET_0 = \frac{0.408\Delta(R_n - G) + \gamma\frac{900}{T+273}u_2(e_s - e_a)}{\Delta + \gamma(1 + 0.34u_2)} \tag{16}$$

where ET_0 is reference evapotranspiration (mm day^{-1}), R_n is net radiation at the crop surface (MJ m^{-2} day^{-1}), G is soil heat flux density (MJ m^{-2} day^{-1}), T is mean daily air temperature at 2 m height (°C), u_2 is wind speed at 2 m height (m s^{-1}), e_s is saturation vapour pressure (kPa), e_a is actual vapour pressure (kPa), e_s-e_a represents the vapour pressure deficit (VPD, kPa), Δ is the slope of the vapour pressure curve (kPa °C^{-1}), and γ is the psychrometric constant (kPa °C^{-1}).

Variations in VPD are therefore inherently captured in ET_0 calculations and directly regulate crop transpiration and soil water depletion rates (an example is shown in Fig. S10). Under higher atmospheric demand, accelerated transpiration leads to more rapid soil moisture depletion, causing the prescribed threshold to be reached earlier and increasing irrigation frequency. Conversely, under lower atmospheric demand, soil water depletion proceeds more slowly and irrigation events are delayed. Consequently, although this study employs fixed, stage-specific soil moisture thresholds, irrigation timing and frequency respond dynamically to atmospheric demand through the coupled soil–plant–atmosphere system dynamics.

Importantly, the optimal stage-specific thresholds ($SMT^{*}_{i,s}$) are derived through nonlinear constrained optimization over a long-term historical climate sequence (2000–2022), which spans a wide range of atmospheric demand conditions, including years with high VPD and elevated evaporative demand. In this sense, the thresholds can be viewed as having been implicitly stress-tested across diverse atmospheric regimes. Consequently, the optimized stage-specific thresholds represent a statistically optimal compromise under historical climate variability, balancing yield risk during high-demand periods against water-saving potential during low-demand conditions.

Spatial upscaling of optimal SMTs

Having obtained site-level optimal thresholds, we then upscaled these point-based results to regional surfaces for spatial analysis. Optimized stage-specific thresholds (SMT^{*}_1–SMT^{*}_4) were interpolated into regional maps using Ordinary Kriging. Station coordinates were reprojected to the target coordinate reference system, and interpolation grids were generated from the study GeoTransform. Following semi-variogram testing, a spherical model was selected, as it is widely used in agricultural and environmental applications for capturing spatial dependence that levels off beyond a finite range (Hengl et al., 2017; Wen et al., 2025). Model parameters (nugget, sill, range) were automatically fitted to the data. The interpolated outputs were masked to cotton cropland and exported as single-band GeoTIFFs with consistent coordinate reference system and 5′ (~10 km) resolution.

2.6. Regional-scale simulation in Xinjiang

Regional simulations were performed for 1337 cotton cropland grids in Xinjiang, with all 15 cotton cultivars simulated in each grid. Grid-level results were calculated as the mean of the cultivar-specific simulations. To ensure consistency and comparability, all non-climatic inputs and model parameters were kept constant between the historical and future simulations. These inputs included planting dates, crop parameters, and management practices, all of which were based on the validation values described in previous sections. Soil properties, derived from the SoilGrids dataset, were treated as static inputs, as they change slowly over time and are unlikely to vary significantly within the simulation period.

The only inputs that varied between the historical and future simulations were the climate drivers, including temperature, precipitation, and atmospheric CO_2 concentration. Historical simulations used ERA5-Land reanalysis data, while future projections were based on statistically downscaled NEX-GDDP-CMIP6 climate scenarios. Under these consistent settings, the AquaCrop model was used to simulate seed cotton yield, seasonal irrigation amount, and IWP under both the CIS and SMTIS. This approach ensured that any differences in simulation outcomes between the historical and future periods could be attributed solely to the effects of climate change.

2.7. Evaluation of SMTIS benefits and its driving factors

To evaluate SMTIS benefits relative to CIS, we calculated changes in seasonal irrigation amount, irrigation water productivity, and economic benefits:

$$\Delta Irrigation = Irrigation_{SMTIS} - Irrigation_{CIS} \tag{17}$$

$$\Delta IWP = IWP_{SMTIS} - IWP_{CIS} \tag{18}$$

$$EB = \Delta Yield \times CP - \Delta Irrigation \times WP \quad (19)$$

where ΔIrrigation is the change in seasonal irrigation amount (m^3 ha^{-1}), ΔIWP is the change in irrigation water productivity (kg m^{-3}), and EB is the net economic benefit (CNY ha^{-1}) of SMTIS relative to CIS. The cotton price (CP), representing the market price of seed cotton, was set at 7.20 CNY kg^{-1} , while the water price (WP), representing the cost of irrigation water, was set at 0.407 CNY m^{-3} (Dong et al., 2024; Yang and Ma, 2024).

To identify the key climatic and soil drivers of SMTIS effectiveness, we employed an ordinary least squares regression with standardized predictors and response variables (Freedman, 2009).The predictors included mean growing season temperature (Tavg), precipitation (Prcp), ET_0, GDD, soil texture components (silt and clay), bulk density (Bdod), and soil organic carbon (SOC). To minimize multicollinearity among predictors, we adopted a correlation-based screening approach, excluding variables with Pearson correlation coefficients $|r| \geq 0.8$ (Chen et al., 2025a; Jayasinghe and Kumar, 2019; Yu et al., 2022). As shown in Fig. S7, sand content was strongly negatively correlated with silt (r = -0.85) and therefore excluded, while either Tavg or GDD was retained because of their near-perfect positive correlation (r = 0.95). The remaining predictors all exhibited $|r| \leq 0.6$, indicating acceptable levels of intercorrelation for regression analysis.

The response variable Y in Eq. (20) represents one of the four metrics comparing SMTIS with CIS: change in seed cotton yield, change in irrigation water amount, change in IWP, or EB. Each response was modeled separately. To capture temporal heterogeneity, interaction terms between predictors and simulation periods (historical, 2040 s, 2070 s) were included. All predictors and responses were standardized to allow comparability of effect sizes. The regression model was expressed as:

$$Y = \sum_i X_i \times Period_j + \varepsilon \quad (20)$$

where X_i denotes standardized predictors, $Period_j$ represents simulation periods, and interaction terms capture the marginal contributions of predictors within each period. Standardized regression coefficients were extracted for each period, and mean values across periods were calculated to reveal overall trends.

To facilitate transparency, reproducibility, and future reuse, the optimization framework integrating AquaCrop with the SLSQP algorithm and the accompanying geospatial data processing scripts has been publicly released. The codes are available at https://github.com/SmartAG-NWAFU/xinjiang-cotton-smt-irrigation.

3. Results

3.1. Model calibration and validation

The AquaCrop model was calibrated and validated using observed canopy cover, aboveground biomass, and seed cotton yield across the 10 experimental sites (Fig. 4). Canopy cover was reproduced with high accuracy ($R^2 = 0.94$, RMSE = 7.45%, d = 0.99 for calibration; $R^2 = 0.95$, RMSE = 6.69%, d = 0.99 for validation). Aboveground biomass was also well captured ($R^2 = 0.95$, RMSE = 1.29 t ha^{-1}, d = 0.99 for calibration; $R^2 = 0.91$, RMSE = 1.78 t ha^{-1}, d = 0.98 for validation). Seed cotton yield was simulated with acceptable accuracy, though less precise than canopy cover and biomass ($R^2 = 0.88$, RMSE = 0.36 t ha^{-1}, d = 0.97 for calibration; $R^2 = 0.80$, RMSE = 0.38 t ha^{-1}, d = 0.96 for validation). Overall, these results confirm that AquaCrop can reliably reproduce cotton growth and yield dynamics in Xinjiang, providing a robust foundation for subsequent optimization and scenario analyses.

3.2. Optimized spatial thresholds for SMTIS

After model validation, stage-specific soil moisture thresholds were optimized at each site and interpolated into regional maps (Fig. 5). The optimized threshold during the emergence stage (SMT_1^*) remained relatively uniform across Xinjiang, clustering around 62–63% of TAW (mean = 62.6%). During canopy growth, the optimized threshold (SMT_2^*) increased slightly, ranging from 64% to 72% of TAW (mean = 67.9%), reflecting the greater water requirements associated with rapid vegetative expansion. The threshold during the maximum canopy cover stage (SMT_3^*) exhibited the highest spatial variability, spanning 74–100% of TAW (mean = 81.6%), indicating strong spatial heterogeneity in mid-season water demand. By contrast, the threshold during senescence (SMT_4^*) decreased and converged toward lower values, averaging around 57% of TAW (mean = 57.4%), consistent with declining water demand in the late growth stage. Overall, these results demonstrate that irrigation thresholds are most sensitive and spatially variable during the maximum canopy cover stage, underscoring the critical importance of mid-season water management for optimizing irrigation water productivity at the regional scale.

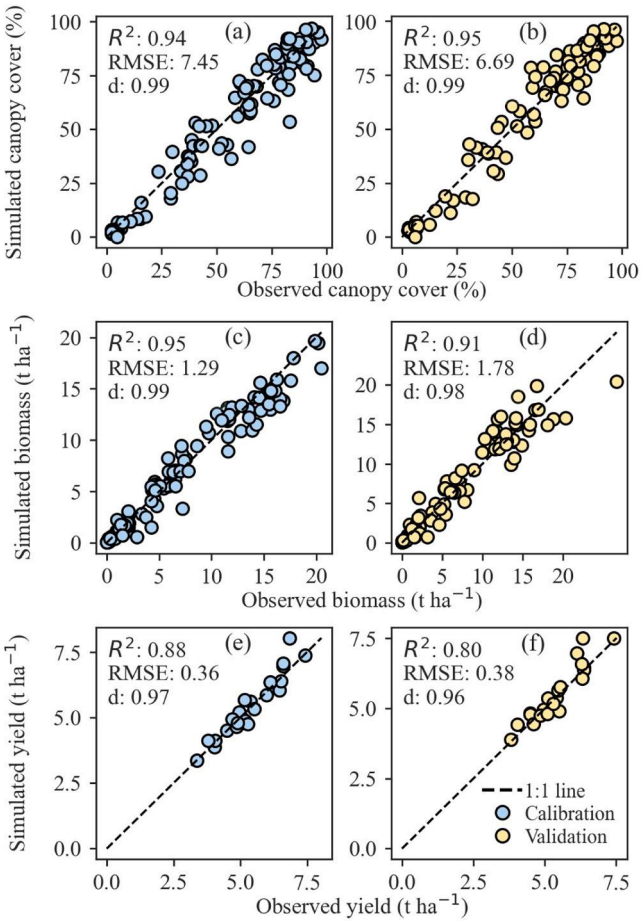

Fig. 4. Comparison between observed and simulated values of canopy cover, aboveground biomass, and seed cotton yield during model calibration (left panels) and validation (right panels). The black dashed lines represent the 1:1 line. Biomass refers to aboveground biomass, and yield refers to seed cotton yield. Model performance was evaluated using the coefficient of determination (R^2), root mean square error (RMSE), and the index of agreement (d). Model performance is generally considered acceptable when $R^2 > 0.5$ or $d > 0.65$, with RMSE values approaching zero indicating high simulation accuracy.

3.3. Effects of SMTIS on yield, irrigation and water productivity

To further assess the performance of the SMTIS and its potential advantages over the CIS, we analyzed their impacts on seed cotton yield, seasonal irrigation water amount and IWP under both historical and

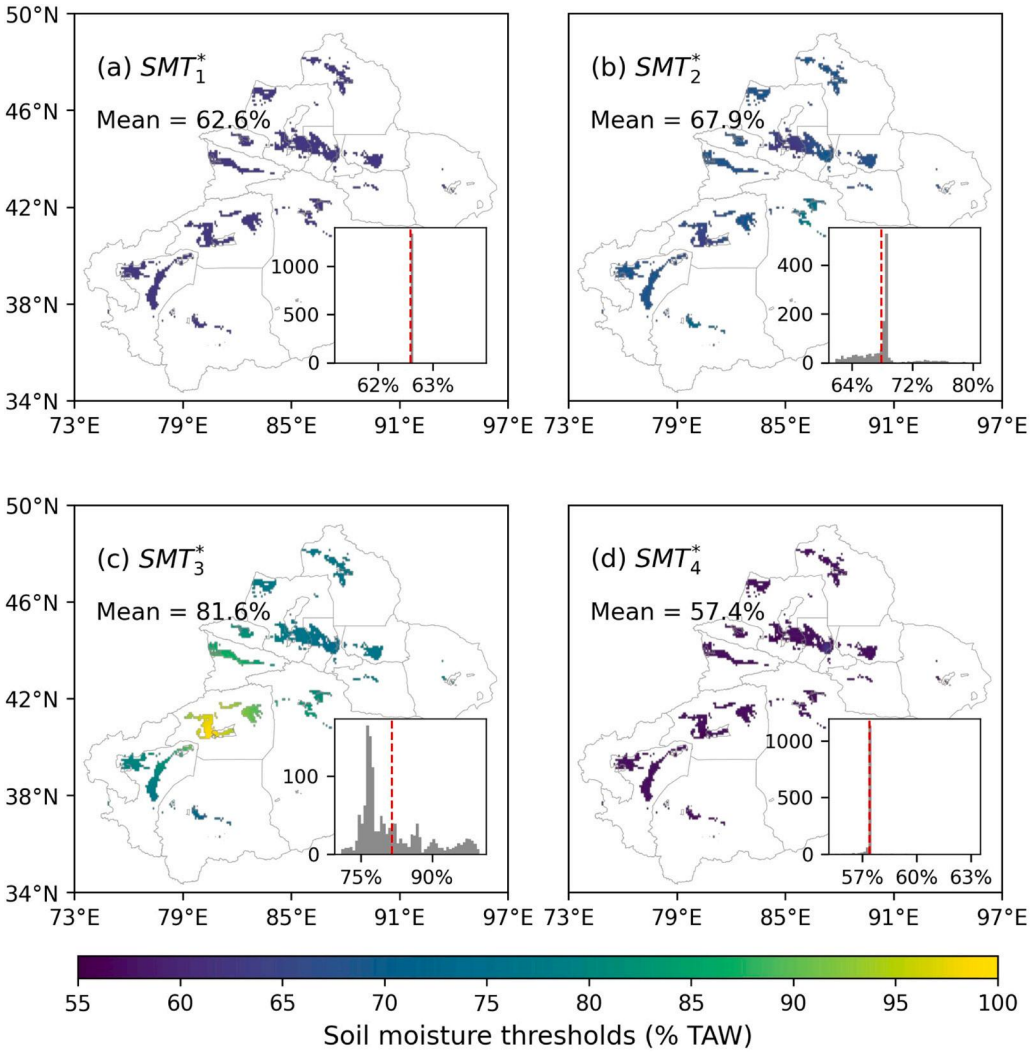

Fig. 5. Optimized spatially soil moisture thresholds for cotton at four growth stages: emergence (SMT_1^*), canopy growth (SMT_2^*), maximum canopy cover (SMT_3^*), and canopy senescence (SMT_4^*). Thresholds are expressed as percentages of total available water (TAW). Insets show frequency distributions of thresholds, and the red dashed line indicates the mean value for each stage.

future climate conditions. Figs. S8 and S9 present the spatial and temporal patterns of seed cotton yield, irrigation water amount, and IWP under CIS and SMTIS, respectively. Under the CIS, seed cotton yield exhibited a broadly similar spatial distribution across Xinjiang. Irrigation water amount showed a distinct spatial gradient, with higher values in southern Xinjiang (around 700 mm) and lower values in the northern region (around 550 mm). IWP was consistently higher in northern areas than in the south. From a temporal perspective, climate change led to a clear increase in yield, rising from approximately 6.0 t ha^{-1} in the historical period to about 6.9 t ha^{-1} in future scenarios, whereas changes in irrigation water amount and IWP remained relatively small. Under the SMTIS (Fig. S9), the spatial distribution of yield was broadly similar to that under CIS, and IWP remained slightly higher in northern Xinjiang. Spatial differences in irrigation water amount were less pronounced, with values in both regions mostly ranging between 350 and 450 mm. Over time, climate change further increased yield and slightly improved IWP, while irrigation water amount exhibited minimal variation.

Building on these spatial and temporal patterns, we further quantified the relative performance of SMTIS compared with CIS to understand how the optimized irrigation strategy modifies crop production and irrigation water amount (Fig. 6). Cotton yields showed slight reductions in the historical period (0–0.5 t ha^{-1}), but shifted to consistent gains in the future, with the largest increases (0.5–0.92 t ha^{-1}) projected for the 2070 s under SSP5–8.5. Seasonal irrigation amount was consistently reduced. Historically, reductions were concentrated at 200–300 mm, while under future climates the spatial gradient widened: 200–250 mm in northern Xinjiang and 250–300 mm in the south. IWP improved robustly across all scenarios. Increases of 0.5–0.85 kg m^{-3} were observed historically, rising to 0.75–1.0 kg m^{-3} by the 2070 s under SSP5–8.5. Northern Xinjiang generally exhibited stronger improvements than the south, particularly in the historical period.

3.4. Comparative performance of SMTIS and CIS under climate change

Fig. 7 provides an overall comparison of SMTIS and CIS across historical and future climate scenarios. In the historical period, cotton seed yields under the two strategies were nearly identical. Under future climates, however, SMTIS delivered clear advantages, with mean yield gains reaching 0.65 t ha^{-1} by the 2070 s under SSP5–8.5 (Fig. 7a). In contrast, irrigation and IWP exhibited complementary responses. Seasonal irrigation under SMTIS was consistently lower, averaging 247 mm less than CIS across all periods (Fig. 7b). These reductions directly translated into efficiency gains, with mean IWP increasing by 0.83 kg m^{-3} relative to CIS (Fig. 7c). The consistency across six CMIP6 climate models—evidenced by narrow interquartile ranges and close agreement of multi-model means—underscores the robustness of these

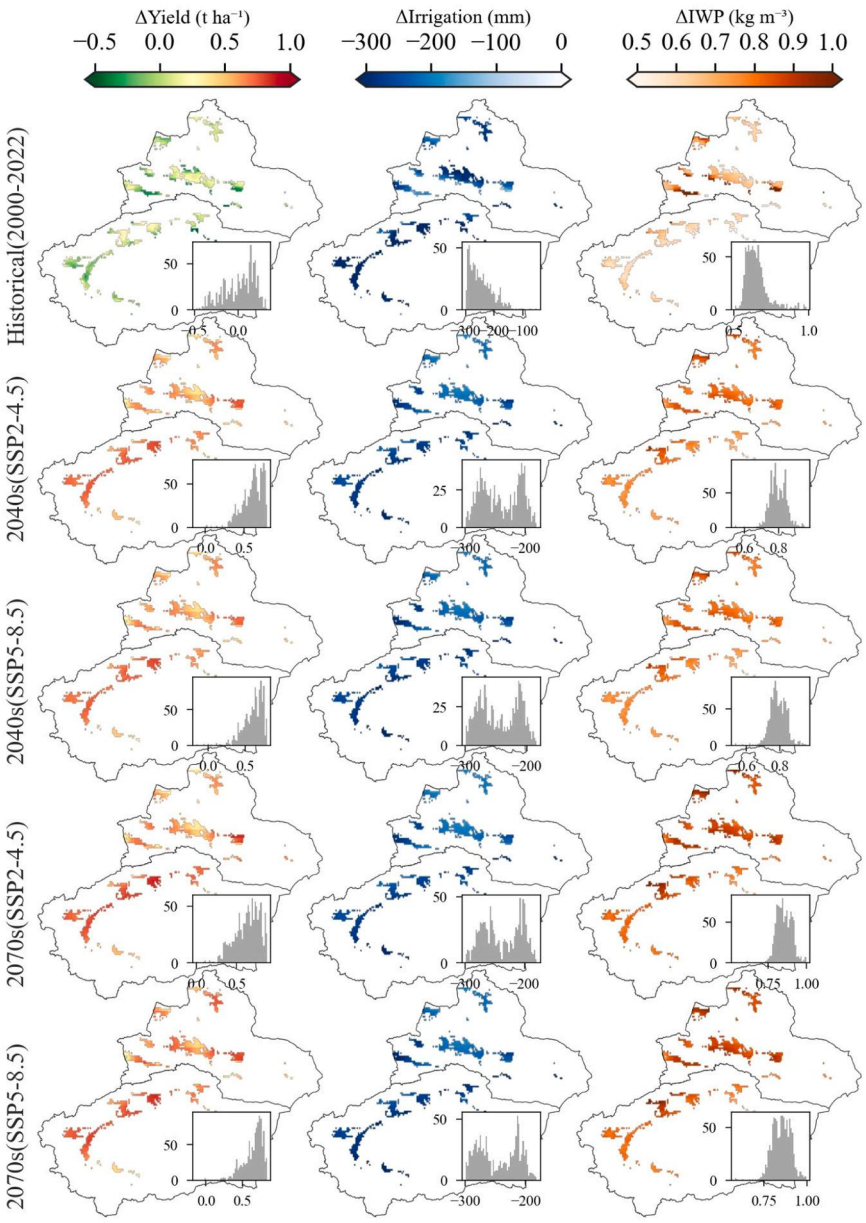

Fig. 6. Changes in cotton yield (ΔYield), seasonal irrigation amount (ΔIrrigation) and irrigation water productivity (ΔIWP) under soil moisture threshold–based irrigation strategy relative to conventional irrigation strategy in Xinjiang. Results are shown for the historical period (2000–2022) and future scenarios (2040 s: 2031–2050; 2070 s: 2061–2080) under SSP2-4.5 and SSP5-8.5. Insets show site-level frequency distributions for each indicator.

outcomes. Overall, SMTIS emerges as a reliable strategy for reducing water use while simultaneously enhancing productivity under varying climate conditions.

3.5. *Drivers of SMTIS effectiveness*

Fig. 8 presents the regression coefficients of climatic and soil predictors for SMTIS effectiveness, including average effects across all simulation periods (Fig. 8a) and period-specific effects for the historical period, the 2040 s, and the 2070 s (Fig. 8b-d). Overall, climatic variables exerted stronger influences than soil properties. Higher ET_0 was strongly and negatively associated with ΔIrrigation (−0.82), indicating greater irrigation savings under high evaporative demand. Precipitation showed negative coefficients with both ΔYield (−0.34) and EB (−0.28), suggesting that drier regions benefited more in terms of yield and profitability. In contrast, precipitation was positively related to ΔIWP (0.36), meaning that wetter regions achieved larger improvements in irrigation water productivity. Among soil factors, silt content was positively associated with ΔIWP (0.17) and EB (0.11).

Period-specific effects revealed clear shifts over time. For ΔYield, the coefficient of Tavg was positive in the historical period (0.24) but became negative in the 2040 s (−0.06) and 2070 s (−0.08). Likewise, ET_0 had a negative coefficient with ΔYield historically (−0.46) but turned positive in the future (0.03 and 0.05 in the 2040 s and 2070 s). Soil effects also strengthened: the coefficient of silt with ΔYield rose from 0.02 in the historical period to 0.12 in the 2070 s, while bulk density increased from −0.02–0.11 over the same interval.

Together, these results demonstrate that SMTIS effectiveness is co-regulated by climate and soil. Climate variables dominate under current conditions, whereas soil properties gain importance as climate stress intensifies. This pattern is conceptually summarized in Fig. S11, which highlights the temporal shift from climate-dominated to more soil-influenced regulation of SMTIS performance. These findings suggest that prioritizing SMTIS in regions with high evaporative demand and

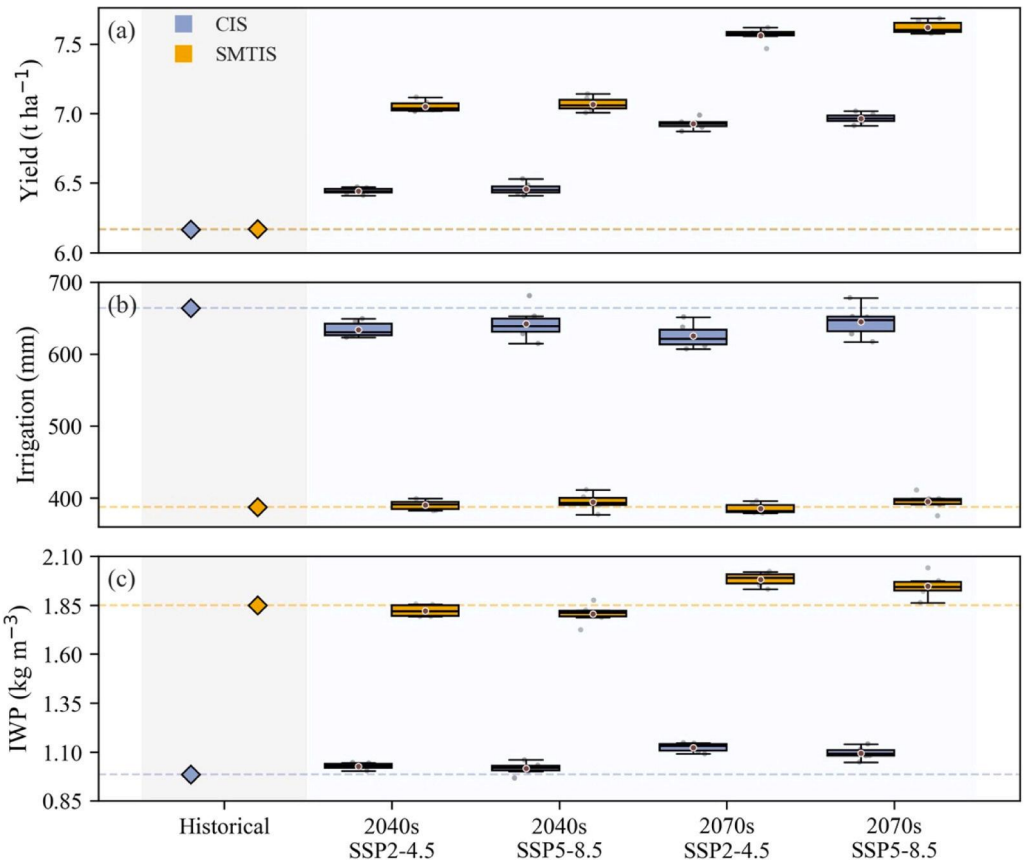

Fig. 7. Comparative performance of soil moisture threshold–based irrigation strategy (SMTIS) and conventional irrigation strategy (CIS) for cotton production in Xinjiang under climate change scenarios. Panels show (a) cotton seed yield, (b) seasonal irrigation amount and (c) irrigation water productivity across the historical period (2000–2022), the 2040 s (2031–2050), and the 2070 s (2061–2080). Results are presented for six CMIP6 climate models under SSP2-4.5 and SSP5-8.5, with red points indicating multi-model means.

favorable soil conditions will maximize water-saving and economic benefits.

4. Discussion

Xinjiang, one of the world's largest cotton-producing regions, faces severe water scarcity, making efficient irrigation essential (Chen et al., 2025b; Geng et al., 2023). In this study, we combined the AquaCrop model with the SLSQP algorithm and Kriging interpolation to design a soil moisture threshold-based irrigation strategy (SMTIS). Once validated, SMTIS demonstrated that optimized thresholds could lower seasonal irrigation amount by 200–300 mm, while keeping yields stable in the past and improving them under future climates. Yield gains were most pronounced in the 2070 s under the SSP5–8.5 scenario, reaching up to 0.92 t ha^{-1} , alongside notable improvements in irrigation water productivity (IWP) ranging from 0.75 to 1.0 kg m^{-3} . Overall, SMTIS offers a robust and climate-resilient pathway to improve water-use efficiency, sustain cotton yields, and support water management in arid cotton-growing regions.

4.1. Optimized SMTIS thresholds

The optimized soil moisture thresholds exhibited clear stage-specific differences, consistent with cotton's physiological water requirements. In this study, the average optimized thresholds, expressed as percentages of total available water (TAW), were 62.1% at emergence, 67.0% at canopy growth, 81.9% at maximum canopy cover, and 57.1% at canopy senescence (Fig. 5). This progression reflects cotton's dynamic water demand: moderate during early vegetative growth, peaking during reproductive development when boll formation is highly sensitive to stress, and declining during maturation as assimilates are redirected to fiber development (Dong et al., 2000; Li et al., 2019). Previous studies based on field capacity reported broadly similar ranges, such as 55–80% FC across stages (Li et al., 2013; Pan et al., 2019; Wang et al., 2018). Compared with these FC-based guidelines, our TAW-based results provide a more systematic and spatially explicit framework, enabling thresholds to be dynamically adapted to environmental conditions across Xinjiang.

Beyond the stage-specific averages, thresholds also displayed substantial spatial variability, indicating that optimal irrigation regimes are shaped by environmental as well as physiological factors. Thresholds at maximum canopy cover showed the widest spread (74–100% of TAW), whereas emergence and canopy senescence thresholds were more narrowly distributed (±3–5%). This variability reflects the joint influence of climate and soil conditions. In southern Xinjiang, where precipitation is scarce and evaporative demand is high, higher thresholds were required to avoid water stress, consistent with findings by He et al. (2020), who reported sharp yield declines when irrigation was delayed below 65–70% FC (about 40–50% TAW). By contrast, in northern Xinjiang, relatively higher rainfall and lower evaporative demand, allowed crops to tolerate lower thresholds without yield penalties. Soil properties reinforced these regional contrasts: sandy soils with low organic matter and high bulk density, common in the south, dried rapidly and necessitated earlier irrigation, while loamy soils with higher water-holding capacity in the north buffered short-term deficits and permitted lower thresholds without yield loss (Li et al., 2019; Rui, 2024; Wang et al., 2023). These spatial contrasts demonstrate that climatic aridity and soil properties jointly drive the regional variability of

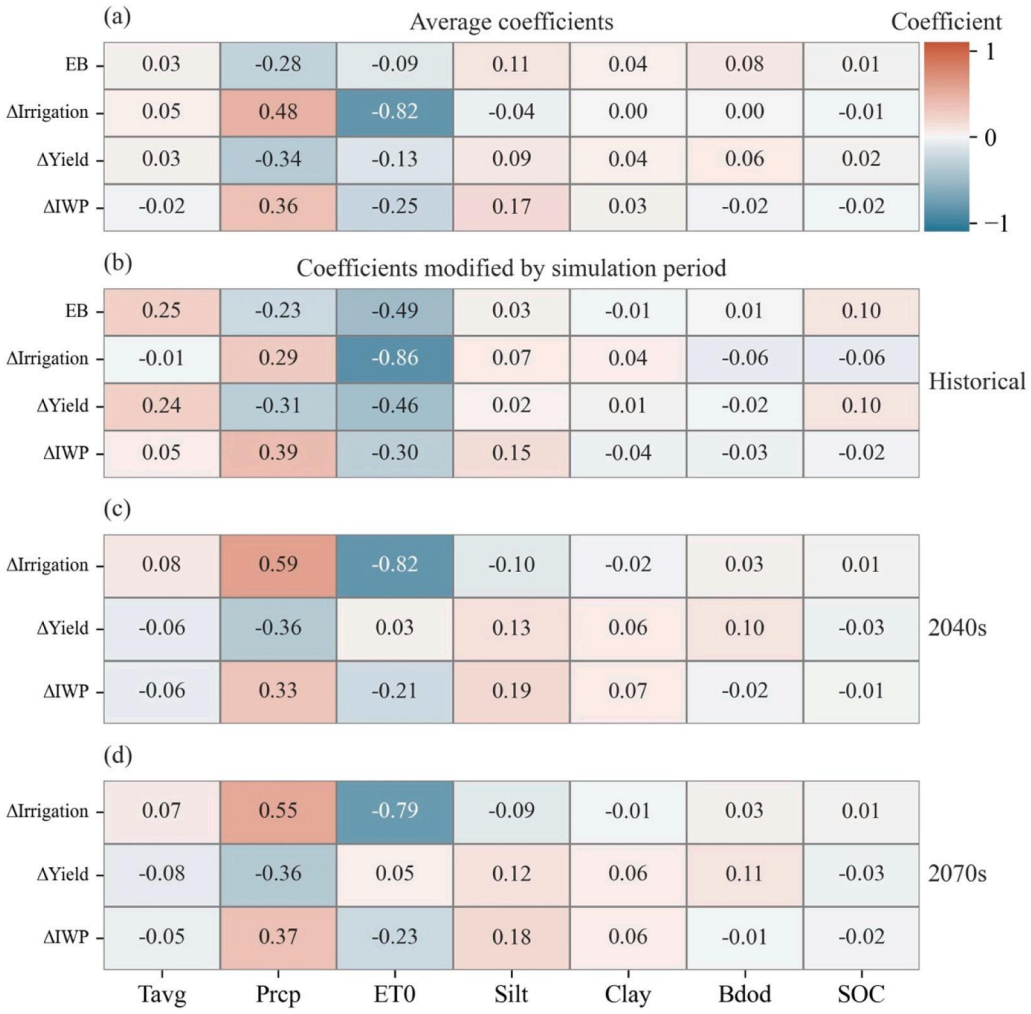

Fig. 8. Regression coefficients of climatic and soil predictors for soil moisture threshold–based irrigation strategy effectiveness. (a) Average coefficients across all simulation periods (historical:2000–2022, 2040 s: 2031–2050, and 2070 s: 2061–2080); (b–d) Period-specific coefficients. Tavg: mean growing season temperature; Prcp: precipitation; ET_0: potential evapotranspiration; GDD: growing degree days; Silt and Clay: soil texture components; Bdod: bulk density; SOC: soil organic carbon. Response variables include ΔYield (yield change), ΔIrrigation (irrigation change), ΔIWP (change in irrigation water productivity), and EB (change in economic benefits), each expressed relative to conventional irrigation.

optimized irrigation thresholds, indicating that uniform thresholds are unsuitable across Xinjiang. Instead, regionally tailored, stage-specific threshold maps are essential for irrigation management.

4.2. Climatic and soil drivers of SMTIS effectiveness

Climatic variables emerged as the dominant drivers of SMTIS effectiveness across Xinjiang. Higher reference evapotranspiration (ET_0) was strongly associated with greater irrigation savings, indicating that under high evaporative demand conditions the optimized strategy delivers substantial water-saving benefits. Precipitation showed an inverse relationship with yield gains and economic benefits, with drier regions exhibiting larger improvements in seed cotton yield and profitability. However, the response of IWP differed slightly, showing greater improvements in wetter regions (Fig. 8). This pattern aligns with previous findings that deficit or threshold-based irrigation strategies are most effective in arid and semi-arid environments, where each unit of irrigation water has higher marginal value (Fanuel et al., 2018; Plumblee et al., 2019). Collectively, these results confirm that climatic conditions—particularly evaporative demand and rainfall—largely determine where SMTIS provides the greatest comparative advantage.

Although secondary at present, soil factors also influenced SMTIS outcomes, and their importance is likely to increase under future climate stress. Soil texture, bulk density, and SOC regulate water retention and infiltration, thereby shaping how threshold-based irrigation translates into plant-available water. Loamy soils with higher organic matter buffer short-term deficits, allowing lower thresholds without yield penalty. In contrast, sandy soils with low SOC and high bulk density dry rapidly and require earlier or more frequent irrigation triggers (Dong et al., 2000; Li et al., 2019; Rui, 2024). Yu et al. (2020) similarly found that deficit irrigation performed best in areas with < 200 mm rainfall and coarse-textured soils, particularly under border and furrow systems, underscoring the interaction between soil conditions and irrigation strategy.

From a management perspective, SMTIS should be prioritized in regions with high evaporative demand and scarce rainfall, such as the oases of southern Xinjiang, where water-saving and economic benefits are greatest. At the same time, soil properties must be considered to avoid delayed irrigation in sandy soils and excessive irrigation in loamy or clay soils. In short, climate determines where SMTIS is most beneficial, while soil properties determine how it should be tailored locally, providing a dual basis for precision irrigation in Xinjiang and other arid regions.

4.3. Application potential of SMTIS in Xinjiang

The application of the SMTIS holds significant potential for improving irrigation water management in Xinjiang. Our results indicate that, on average, SMTIS consistently reduced irrigation water use by 200–300 mm per season across all periods and regions, while maintaining or even improving yields and IWP, with gains ranging from 0.5 to 1.0 kg m^{-3} . Economic benefits were assessed for the historical period (2000–2022), as shown in Fig. 9. The results indicate that approximately 17.36% of the cotton-growing areas experienced slight economic losses, ranging from 0 to 1.99×10^{3} CNY ha^{-1} . In contrast, the majority of regions (82.64%) exhibited positive economic gains between 0 and 3.0×10^{3} CNY ha^{-1} . Overall, the mean economic benefit across all regions reached 1.27×10^{3} CNY ha^{-1} , highlighting the general economic advantage of SMTIS over conventional irrigation under historical climate conditions.

The effectiveness of SMTIS varied regionally, with particularly notable results in southern Xinjiang, where water scarcity and high evaporative demand present significant challenges. This region is also highly vulnerable to the impacts of climate change, which is expected to exacerbate drought stress (Kuang et al., 2024). As a result, SMTIS was especially effective in conserving water and improving crop yields in these areas. In contrast, northern Xinjiang showed smaller, but still positive, improvements, suggesting that SMTIS could first be implemented in the water-scarce southern oases before expanding to the less stressed northern regions.

Notably, improvements in yield and IWP were even more pronounced under the high-emission scenario, as shown in Fig. S9. Two factors help explain why using less water can still boost production in future climates. First, elevated atmospheric CO_2 (Fig. S2) concentrations enhance photosynthesis and increase water-use efficiency in cotton (Jans et al., 2021). Second, a soil-moisture-threshold irrigation approach allows water to be applied only when root-zone water drops below a critical threshold, improving the timing and distribution of irrigation; experiments have shown that such thresholds can maximize irrigation water-use efficiency (Li et al., 2019). These mechanisms enable SMTIS to deliver higher yields and profits despite reduced water inputs, underscoring its potential as a climate-resilient strategy for sustaining cotton production. Furthermore, the practicality of SMTIS for large-scale implementation is underpinned by its reliance on thresholds optimized under historical climate variability. This design ensures that the strategy remains robust and operationally simple—qualities that are essential for the extensive cotton production systems in Xinjiang. By prioritizing long-term stability, SMTIS offers a solid and scalable framework for formulating regional irrigation strategies.

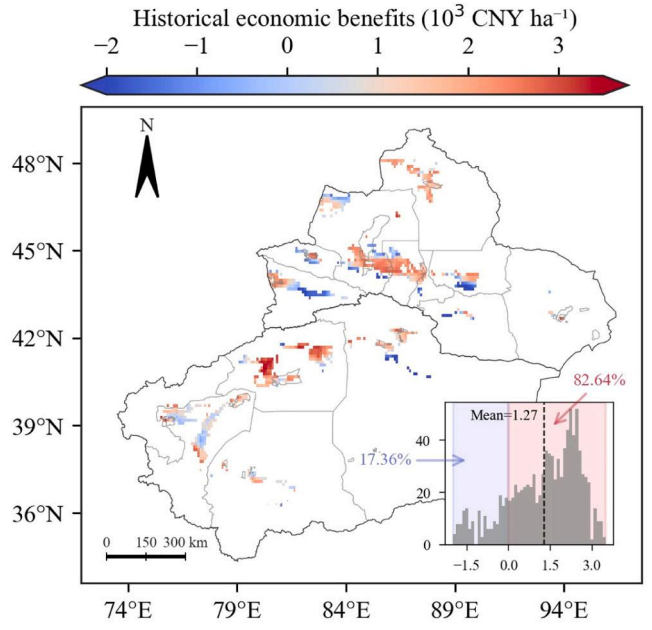

Fig. 9. Spatial distribution of historical economic benefits (10^3 CNY ha^{-1}) during 2000–2022 under the soil moisture threshold–based irrigation strategy compared with the conventional irrigation strategy across Xinjiang. Insets show the frequency distribution of economic benefits, with the black dashed line indicating the mean value.

However, it is acknowledged that SMTIS may not represent the optimal irrigation decision at the daily scale, as crop water stress can differ even under similar soil moisture conditions when atmospheric demand fluctuates. Dynamic threshold approaches, which directly respond to short-term variations in vapor pressure deficit or evaporative demand, could offer advantages in highly instrumented precision irrigation systems (Zhang et al., 2021). Therefore, when applying SMTIS for field-level irrigation guidance, local calibration and small-scale validation are recommended, with due consideration of cotton cultivar characteristics, soil hydraulic properties, and prevailing atmospheric conditions.

Looking forward, future work could build upon the current SMTIS framework by introducing a hierarchical two-layer control scheme. In such a system, the stage-specific thresholds optimized by SMTIS would serve as a baseline control layer to ensure long-term robustness and water productivity, while an upper-layer daily adjustment module could be incorporated to fine-tune irrigation timing in response to short-term atmospheric demand indicators. This hybrid approach has the potential to enhance the applicability of SMTIS in precision irrigation contexts without compromising its scalability and suitability for data-limited production environments.

4.4. Limitations and future research

While this study provides a robust framework and promising results, there are several limitations that should be considered. First, the optimization process in this study prioritized yield and irrigation water productivity, without explicitly considering other critical factors such as fiber quality, operational farm-level costs (e.g., pumping energy, labor, and equipment), or broader environmental impacts (Li et al., 2025; Rui, 2024). Future research could adopt more multi-objective frameworks to balance water savings, yield, quality and environmental considerations.

Second, economic analysis in this study was intentionally restricted to the historical period. Projecting specific economic returns several decades into the future would require assumptions about cotton prices, water costs, trade policies, subsidies, and technological developments, all of which are highly uncertain and beyond the predictive scope of crop modeling. Consequently, future scenario analyses in this study focus exclusively on biophysical indicators, such as irrigation water use, yield, and irrigation water productivity, rather than long-term economic valuation.

Third, it is important to distinguish the strategic focus of this study from real-time irrigation management. We acknowledge that recent advances have successfully integrated remote sensing data with crop models to correct state variables and capture intra-field variability, thereby enhancing field-scale phenology characterization and within-season decision support (Wang et al., 2022). However, as our study aimed to evaluate the resilience of irrigation strategies under multi-decadal climate variability and future warming scenarios, it necessitated a reliance on process-based modeling underpinned by rigorous experimental calibration and validation. Consequently, the optimized SMTIS derived here serves as a strategic baseline. Future implementation could effectively bridge these approaches by using remote sensing to spatially characterize real-time water stress dynamics and guide irrigation scheduling based on the robust thresholds identified in this study.

Finally, a limitation arises from the reliance on standard 2-m height meteorological data for irrigation scheduling. Although widely used, these data may not accurately reflect canopy-level conditions, especially

under water stress when temperatures at the crop canopy can differ substantially from air temperatures. The relationship between air and canopy temperatures is dynamic, influenced by various environmental factors (Morales-Santos and Nolz, 2023). This discrepancy is particularly important under future climate scenarios where temperature increases and water stress could shift this relationship in ways that current models cannot fully capture. While this is a known limitation of crop models, future work should explore ways to incorporate canopy temperature data or refine models to better address crop water stress under changing climates.

5. Conclusions

This study integrates the AquaCrop model with a nonlinear optimization framework to evaluate the impacts of a soil moisture threshold–based irrigation strategy (SMTIS) on cotton yield and irrigation water requirements under historical and future climate conditions. On average, SMTIS reduced seasonal irrigation by 200–300 mm, while maintaining or even enhancing yields, resulting in irrigation water productivity improvements ranging from 0.5 to 1.0 kg m^{-3} across all periods. During the historical period, SMTIS generated a mean economic benefit of 1.27×10^{3} CNY ha^{-1} across all regions. The optimized soil moisture thresholds demonstrated clear stage-specific and spatial variability, with the maximum canopy cover stage being the most sensitive, and southern Xinjiang requiring higher thresholds due to harsher environmental conditions. Climatic variables emerged as the dominant drivers of SMTIS effectiveness, while soil properties played a secondary, yet increasingly important role under future climate scenarios. Overall, this study presents a robust and climate-resilient irrigation strategy for Xinjiang and other arid cotton-growing regions, offering a practical solution to sustain cotton production while enhancing water-use efficiency and profitability in the face of growing climate and water challenges.

CRediT authorship contribution statement

Genghong Wu: Writing – original draft, Supervision, Formal analysis, Conceptualization. **Mohamed Amine Benaly:** Writing – review & editing, Methodology. **Changqing Yan:** Writing – review & editing. **Hao Feng:** Writing – review & editing. **Gang Zhao:** Writing – original draft, Supervision, Formal analysis, Conceptualization. **Qiang Yu:** Writing – review & editing, Supervision. **Yadong Liu:** Writing – review & editing. **Qiuxiang Tang:** Writing – review & editing. **Bin Chen:** Writing – original draft, Visualization, Software, Methodology, Formal analysis, Conceptualization. **Jianqiang He:** Writing – review & editing. **Linjia Yao:** Writing – original draft, Visualization, Software, Methodology, Formal analysis, Conceptualization. **Dongyan Zhang:** Writing – review & editing. **Jie Bai:** Writing – review & editing. **Ronghao Guan:** Writing – review & editing. **Yi Li:** Writing – review & editing.

Declaration of competing interest

We declare that there are no conflicts of interest to declare.

Acknowledgements

The authors acknowledge financial support from the National Natural Science Foundation of China (Grant No. 42101304), the Key Research and Development Program of Shaanxi (Grant No. 2023-ZDLNY-64), the National Modern Agricultural Industry Technology System-Cotton Industry Technology System (CARS-15–13), the Xinjiang Modern Agricultural Industry Technology System-Cotton Industry Technology System (XIARS-03) and the Sanqin Scholars Smart Agriculture Innovation Team. We also extend our appreciation to the two anonymous reviewers, whose thoughtful comments greatly improved the manuscript.

Appendix A. Supporting information

Supplementary data associated with this article can be found in the online version at doi:10.1016/j.eja.2026.128152.

Data availability

Data will be made available on request.

References

Allen, R.G., Pereira, L.S., Raes, D., Smith, M., 1998. Crop evapotranspiration-Guidelines for computing crop water requirements-FAO Irrigation and drainage paper 56. Fao, Rome 300, D05109.

Bai, Z., Xie, C., Yu, J., Bai, W., Pei, S., Li, Y., Li, Z., Zhang, F., Fan, J., Yin, F., 2024. Effects of irrigation and nitrogen levels on yield and water-nitrogen-radiation use efficiency of drip-fertigated cotton in south Xinjiang of China. Field Crops Res. 308, 109280. https://doi.org/10.1016/j.fcr.2024.109280.

Chen, B., Zhao, G., Tian, Q., Yao, L., Wu, G., Wang, J., Yu, Q., 2025a. Climate-driven shifts in suitable areas of Alternaria leaf blotch (*Alternaria mali Roberts*) on apples: projections and uncertainty analysis in China. Agric. For. Meteorol. 364, 110464. https://doi.org/10.1016/j.agrformet.2025.110464.

Chen, X., Dong, H., Qi, Z., Gui, D., Ma, L., Thorp, K.R., Malone, R., Wu, H., Liu, B., Feng, S., 2025b. Potential deficit irrigation adaptation strategies under climate change for sustaining cotton production in hyper–arid areas. Agric. Water Manag. 312, 109417. https://doi.org/10.1016/j.agwat.2025.109417.

Copernicus Climate Change Service, 2019. ERA5-Land monthly averaged data from 1950 to present. https://doi.org/10.24381/CDS.68D2BB30.

Dong, P., Xiying, Z., Ru, K., 2000. Effects of water deficit on cotton growth, physiology and yield. Chin. J. Eco-Agric. 8, 52–55.

Dong, X., Zhong, F., Ji, Y., 2024. The impact of water prices on farmers' irrigation water input based on the perspective of factor substitution. Chin. J. Agric. Resour. Reg. Plan. 47, 76–86 https://doi.org/10.%25207621/cjarrp.1005-9121.20240707.

Doorenbos, J., Kassam, A.H., 1970. FAO irrigation and drainage paper. 33 (M). Food and Agrieulture Organization of the United Nations.

Du, Y., Fu, Q., Ai, P., Ma, Y., Pan, Y., Du, Y., Fu, Q., Ai, P., Ma, Y., Pan, Y., 2024. Modeling comprehensive deficit irrigation strategies for drip-irrigated cotton using AquaCrop. Agriculture 14. https://doi.org/10.3390/agriculture14081269.

Fanuel, I.M., Mushi, A., Kajunguri, D., 2018. Irrigation water allocation optimization using multi-objective evolutionary algorithm (MOEA) – a review. Int. J. Simul. Multidisci. Des. Optim. 9, A3. https://doi.org/10.1051/smdo/2018001.

Fereres, E., Soriano, M.A., 2007. Deficit irrigation for reducing agricultural water use. J. Exp. Bot. 58, 147–159. https://doi.org/10.1093/jxb/erl165.

Freedman, D.A., 2009. Statistical models: theory and practice. cambridge university press.

García-Vila, M., Fereres, E., 2012. Combining the simulation crop model AquaCrop with an economic model for the optimization of irrigation management at farm level. Eur. J. Agron. 36, 21–31. https://doi.org/10.1016/j.eja.2011.08.003.

García-Vila, M., Fereres, E., Mateos, L., Orgaz, F., Steduto, P., 2009. Deficit irrigation optimization of cotton with AquaCrop. Agron. J. 101, 477–487. https://doi.org/10.2134/agronj2008.0179s.

Geng, Q., Zhao, Y., Sun, S., He, X., Wang, D., Wu, D., Tian, Z., 2023. Spatio-temporal changes and its driving forces of irrigation water requirements for cotton in Xinjiang, China. Agric. Water Manag. 280, 108218. https://doi.org/10.1016/j.agwat.2023.108218.

Gong, M., Zhao, F., Zeng, S., Li, C., 2023. An experimental study on local and global optima of linear antenna array synthesis by using the sequential least squares programming. Appl. Soft Comput. 148, 110859. https://doi.org/10.1016/j.asoc.2023.110859.

Guan, R., Li, Y., Jia, Y., Jiang, F., Li, L., 2024. Acidified biochar one-off application for saline-alkali soil improvement: a three-year field trial evaluating the persistence of effects. Ind. Crops Prod. 222, 119972. https://doi.org/10.1016/j.indcrop.2024.119972.

Guan, R., Li, Y., Jia, Y., Jiang, F., Li, L., Biswas, A., Siddique, K.H.M., 2025. Dual impact of single acidified biochar application on saline-alkaline soil: short-term salinization risks and persistent nutrient benefits. Soil Tillage Res. 254, 106745. https://doi.org/10.1016/j.still.2025.106745.

He, P., Zhang, F., Fan, J., Hou, X., Liu, X., Zhang, Y., Xue, Z., 2020. Effects of soil moisture regulation on growth, quality and water use of cotton under drip irrigation in Southern Xinjiang. Agric. Res. Arid Areas 38, 39–46. https://doi.org/10.7606/j.issn.1000-7601.2020.04.06.

Hengl, T., Jesus, J.M. de, Heuvelink, G.B.M., Gonzalez, M.R., Kilibarda, M., Blagotić, A., Shangguan, W., Wright, M.N., Geng, X., Bauer-Marschallinger, B., Guevara, M.A., Vargas, R., MacMillan, R.A., Batjes, N.H., Leenaars, J.G.B., Ribeiro, E., Wheeler, I., Mantel, S., Kempen, B., 2017. SoilGrids250m: global gridded soil information based on machine learning. PLOS ONE 12, e0169748. https://doi.org/10.1371/journal.pone.0169748.

Himanshu, S.K., Ale, S., Bordovsky, J., Darapuneni, M., 2019. Evaluation of crop-growth-stage-based deficit irrigation strategies for cotton production in the Southern High Plains. Agric. Water Manag. 225, 105782. https://doi.org/10.1016/j.agwat.2019.105782.

Hu, W., Yao, J., He, Q., Chen, J., 2021. Changes in precipitation amounts and extremes across Xinjiang (northwest China) and their connection to climate indices. PeerJ 9, e10792. https://doi.org/10.7717/peerj.10792.
International Food Policy Research Institute (IFPRI), 2024. Global Spatially-Disaggregated Crop Production Statistics Data for 2020 Version 2.0. https://doi.org/10.7910/DVN/SWPENT.
Jacovides, C.P., Kontoyiannis, H., 1995. Statistical procedures for the evaluation of evapotranspiration computing models. Agric. Water Manag. 27, 365–371. https://doi.org/10.1016/0378-3774(95)01152-9.
Jans, Y., von Bloh, W., Schaphoff, S., Müller, C., 2021. Global cotton production under climate change – Implications for yield and water consumption. Hydrol. Earth Syst. Sci. 25, 2027–2044. https://doi.org/10.5194/hess-25-2027-2021.
Jayasinghe, S.L., Kumar, L., 2019. Modeling the climate suitability of tea [*Camellia sinensis*(L.) O. Kuntze] in Sri Lanka in response to current and future climate change scenarios. Agric. For. Meteorol. 272273 102–117. https://doi.org/10.1016/j.agrformet.2019.03.025.
Jiang, F., Li, N., Gao, Y., Wang, H., Liang, J., Wang, X., Du, J., 2025. Optimizing a water-saving and salt-controlling irrigation strategy for improving cotton yield with the AquaCrop model under mulched drip irrigation in saline-alkali soil. Irrig. Sci. 43, 581–596. https://doi.org/10.1007/s00271-025-01001-4.
Kang, R., 2021. Effects of different nitrogen application rates on cotton yield and environmental effects under "Kuanzaoyou" mode. Chin. Acad. Agric. Sci.
Kelly, T.D., Foster, T., 2021. AquaCrop-OSPy: bridging the gap between research and practice in crop-water modeling. Agric. Water Manag. 254, 106976. https://doi.org/10.1016/j.agwat.2021.106976.
Kuang, N., Hao, C., Liu, D., Maimaitiming, M., Xiaokaitijiang, K., Zhou, Y., Li, Y., 2024. Modeling of cotton yield responses to different irrigation strategies in Southern Xinjiang Region,China. Agric. Water Manag. 303, 109018. https://doi.org/10.1016/j.agwat.2024.109018.
Legates, D.R., McCabe Jr., G.J., 1999. Evaluating the use of "goodness-of-fit" Measures in hydrologic and hydroclimatic model validation. Water Resour. Res. 35, 233–241. https://doi.org/10.1029/1998WR900018.
Li, H., Qi, Z., Gui, D., Zeng, F., 2019. Water use efficiency and yield responses of cotton to field capacity-based deficit irrigation in an extremely arid area of China. Int. J. Agric. Biol. Eng. 12, 91–101. https://doi.org/10.25165/j.ijabe.20191206.4571.
Li, N., Li, Y., Yang, Q., Biswas, A., Dong, H., 2024a. Simulating climate change impacts on cotton using AquaCrop model in China. Agric. Syst. 216, 103897. https://doi.org/10.1016/j.agsy.2024.103897.
Li, X., Zhang, Z., Pan, Z., Sun, G., Li, P., Chen, J., Wang, L., Wang, K., Li, A., Li, J., Zhang, Y., Zhai, M., Zhao, W., Wang, J., Wang, Z., 2025. Demonstrating almost half of cotton fiber quality variation is attributed to climate change using a hybrid machine learning-enabled approach. Eur. J. Agron. 162, 127426. https://doi.org/10.1016/j.eja.2024.127426.
Li, Y., Lei, X.Y., Bai, Y.G., 2013. The effect of different thresholds of soil moisture on yield and water use efficiency of cotton. J. Irrig. Drain. 32, 132–134.
Li, Z., Liu, H., Wang, T., Gong, P., Li, P., Li, L., Bai, Z., 2024b. Deep vertical rotary tillage depths improved soil conditions and cotton yield for saline farmland in South Xinjiang. Eur. J. Agron. 156, 127166. https://doi.org/10.1016/j.eja.2024.127166.
Linker, R., Ioslovich, I., Sylaios, G., Plauborg, F., Battilani, A., 2016. Optimal model-based deficit irrigation scheduling using AquaCrop: a simulation study with cotton, potato and tomato. Agric. Water Manag. 163, 236–243. https://doi.org/10.1016/j.agwat.2015.09.011.
Liu, K., Bo, Y., Li, X., Wang, S., Zhou, G., 2024. Uncovering current and future variations of irrigation water use across china using machine learning. Earth'S. Future 12, e2023EF003562. https://doi.org/10.1029/2023EF003562.
Liu, Y., Wang, Y., Šimůnek, J., Liao, R., 2025. An integrated data assimilation, crop modeling, and multi-objective optimization framework for improving cotton irrigation water use efficiency. Agric. Water Manag. 319, 109774. https://doi.org/10.1016/j.agwat.2025.109774.
Ma, F., Li, M., 2002. A study of effect of water deficit of three period during cotton anthesis on canopy apparent photosynthesis and WUE. Sci. Agric. Sin. (China) 35, 1467–1472.
Madramootoo, C.A., Mortel, G.M.M., 2025. Irrigation water strategies to intensify vegetable production on smallholder farms in Guyana. Irrig. Drain. 74, 738–748. https://doi.org/10.1002/ird.3026.
Mao, X., Zheng, J., Lu, B., Wang, R., Han, W., Harris, P., 2025. Spatiotemporal drought forecasting in Xinjiang's irrigated agriculture: model comparison and multi-source data integration. J. Hydrol. 660, 133483. https://doi.org/10.1016/j.jhydrol.2025.133483.
Meng, L., 2021. Study on effect of irrigation and fertilization regulation and simulation of cotton growth under film-mulched drip irrigation in southern Xinjiang. Northwest A&F University.
Moghbel, F., Aguilar, J., 2025. Identifying the maximum allowable soil moisture depletion to enhance cotton production irrigated by multiple sprinkler irrigation technologies. Kans. Agric. Exp. Station Res. Rep. 11. https://doi.org/10.4148/2378-5977.8718.
Morales-Santos, A., Nolz, R., 2023. Assessment of canopy temperature-based water stress indices for irrigated and rainfed soybeans under subhumid conditions. Agric. Water Manag. 279, 108214. https://doi.org/10.1016/j.agwat.2023.108214.
National Bureau of Statistics of China, 2022. ⟨http://www.stats.gov.cn/⟩.
O'Neill, B.C., Tebaldi, C., van Vuuren, D.P., Eyring, V., Friedlingstein, P., Hurtt, G., Knutti, R., Kriegler, E., Lamarque, J.-F., Lowe, J., Meehl, G.A., Moss, R., Riahi, K., Sanderson, B.M., 2016. The scenario model intercomparison project (ScenarioMIP) for CMIP6. Geosci. Model Dev. 9, 3461–3482. https://doi.org/10.5194/gmd-9-3461-2016.
Pan, J.J., Fu, Q.P., Abudoukayimu, A., Ma, Y.J., 2019. Effects of irrigation limits at bud stage and flowering stage on yield of drip irrigation cotton. Agric. Res. Arid Areas 37, 27–32.
Plumblee, M.T., Dodds, D.M., Krutz, L.J., Catchot Jr, A.L., Irby, J.T., Jenkins, J.N., 2019. Determining the optimum irrigation schedule in furrow irrigated cotton using soil moisture sensors. Crop Forage & Turfgrass Manag. 5, 180047. https://doi.org/10.2134/cftm2018.06.0047.
Poggio, L., de Sousa, L.M., Batjes, N.H., Heuvelink, G.B.M., Kempen, B., Ribeiro, E., Rossiter, D., 2021. SoilGrids 2.0: producing soil information for the globe with quantified spatial uncertainty. SOIL 7, 217–240. https://doi.org/10.5194/soil-7-217-2021.
Raes, D., Steduto, P., Hsiao, T.C., Fereres, E., 2009. AquaCrop—the FAO crop model to simulate yield response to water: II. Main algorithms and software description. Agron. J. 101, 438–447. https://doi.org/10.2134/agronj2008.0140s.
Raes, D., Steduto, P., Hsiao, T.C., 2012. Reference manual AquaCrop (version 4.0). FAO, Rome, Italy.
Ran, Q., Li, M., Peng, F., Du, Y., Shen, Y., Ma, Y., 2025. Multi-objective optimization design of an umbilical cross-sectional layout based on the sequential least squares quadratic programming algorithm. Ocean Eng. 321, 120365. https://doi.org/10.1016/j.oceaneng.2025.120365.
Rötter, R., Hoffmann, M., Koch, M., Müller, C., 2018. Progress in modelling agricultural impacts of and adaptations to climate change. Curr. Opin. Plant Biol. 45, 255–261. https://doi.org/10.1016/j.pbi.2018.05.009.
Rui, G., 2024. Study on suitable soil moisture thresholds for cotton irrigated by drip irrigation under membrane in Northern Xinjiang. Xinjiang Agriculture University.
Sadati, S.K., Speelman, S., Sabouhi, M., Gitizadeh, M., Ghahraman, B., 2014. Optimal irrigation water allocation using a genetic algorithm under various weather conditions. Water 6, 3068–3084. https://doi.org/10.3390/w6103068.
Shao, L., Gong, J., Fan, W., Zhang, Z., Zhang, M., 2022. Cost comparison between digital management and traditional management of cotton fields—evidence from cotton fields in Xinjiang, China. Agriculture 12, 1105. https://doi.org/10.3390/agriculture12081105.
Song, X., Cao, H., He, Z., Ding, B., Yao, N., 2023. Applicability of the Aquacrop model in optimization of irrigation and salt leaching schedule during the reproductive period of cotton in Northern Xinjiang of China. Trans. Chin. Soc. Agric. Eng. 39, 111–122.
Tan, S., Wang, Q., Zhang, J., Chen, Y., Shan, Y., Xu, D., 2018. Performance of AquaCrop model for cotton growth simulation under film-mulched drip irrigation in southern Xinjiang, China. Agric. Water Manag. 196, 99–113. https://doi.org/10.1016/j.agwat.2017.11.001.
Thorp, K.R., 2020. Long-term simulations of site-specific irrigation management for Arizona cotton production. Irrig. Sci. 38, 49–64. https://doi.org/10.1007/s00271-019-00650-6.
Thrasher, B., Wang, W., Michaelis, A., Melton, F., Lee, T., Nemani, R., 2022. NASA global daily downscaled projections, CMIP6. Sci. Data 9, 262. https://doi.org/10.1038/s41597-022-01393-4.
Todorovic, M., Albrizio, R., Zivotic, L., Saab, M.-T.A., Stöckle, C., Steduto, P., 2009. Assessment of AquaCrop, CropSyst, and WOFOST models in the simulation of sunflower growth under different water regimes. Agron. J. 101, 509–521. https://doi.org/10.2134/agronj2008.0166s.
Wang, F., Wang, Z., Zhang, J., Li, W., 2018. Effects of moisture sensor location and irrigation threshold on physiological index and yield of cotton under mulch drip irrigation. Water Sav. Irrig. 14–19.
Wang, F., Fu, Q., Hong, M., Tang, W., Su, L., Zhu, D., Wang, Q., Wang, F., Fu, Q., Hong, M., Tang, W., Su, L., Zhu, D., Wang, Q., 2025. Optimization of cotton field irrigation scheduling using the aquacrop model assimilated with UAV remote sensing and particle swarm optimization. Agriculture 15. https://doi.org/10.3390/agriculture15171815.
Wang, J., Li, J., Guan, H., 2016. Modeling response of cotton yield and water productivity to irrigation amount under mulched drip irrigation in North Xinjiang. Trans. Chin. Soc. Agric. Eng. 32, 62–68.
Wang, Y., Huang, D., Zhao, L., Shen, H., Xing, X., Ma, X., 2022. The distributed CERES-Maize model with crop parameters determined through data assimilation assists in regional irrigation schedule optimization. Comput. Electron. Agric. 202, 107425. https://doi.org/10.1016/j.compag.2022.107425.
Wang, Y., Chen, J., Wu, F., Yang, B., Han, Y., Feng, L., Wang, Z., Li, X., Lei, Y., Xiong, S., Wang, G., Zhi, X., Li, Y., 2023. Optimizing plant type structure to adjust the temporal and spatial distribution of water consumption and promote the growth and yield formation of cotton. Eur. J. Agron. 147, 126850. https://doi.org/10.1016/j.eja.2023.126850.
Wen, X., Luo, W., Yang, X., Li, F., Zhang, Z., 2025. Comparative analysis of soil organic carbon across different land types in plateau wetlands using Kriging interpolation based on spatial heterogeneity. PLOS ONE 20, e0328246. https://doi.org/10.1371/journal.pone.0328246.
Wu, L., 2015. Coupling effect of water and fertilizer under fertigation and simulation growth of cotton in Xinjiang. Northwest A&F University.
Xiao, C., Ji, Q., Zhang, F., Li, Y., Fan, J., Hou, X., Yan, F., Liu, X., Gong, K., 2023. Effects of various soil water potential thresholds for drip irrigation on soil salinity, seed cotton yield and water productivity of cotton in northwest China. Agric. Water Manag. 279, 108172. https://doi.org/10.1016/j.agwat.2023.108172.
Yang, C., Ma, Q., 2024. Impact of agricultural subsidies on Xinjiang cotton irrigation water efficiency: the mediating effect of farmers' arable land operation scale. J. Agric. Resour. Environ. 41, 1220.
Yu, L., Zhao, X., Gao, X., Siddique, K.H.M., 2020. Improving/maintaining water-use efficiency and yield of wheat by deficit irrigation: a global meta-analysis. Agric. Water Manag. 228, 105906. https://doi.org/10.1016/j.agwat.2019.105906.

Yu, X., Tao, X., Liao, J., Liu, S., Xu, L., Yuan, S., Zhang, Z., Wang, F., Deng, N., Huang, J., Peng, S., 2022. Predicting potential cultivation region and paddy area for ratoon rice production in China using Maxent model. Field Crops Res. 275, 108372. https://doi.org/10.1016/j.fcr.2021.108372.

Zhang, C., Xie, Z., Wang, Q., Tang, M., Feng, S., Cai, H., 2022. AquaCrop modeling to explore optimal irrigation of winter wheat for improving grain yield and water productivity. Agric. Water Manag. 266, 107580. https://doi.org/10.1016/j.agwat.2022.107580.

Zhang, D., Luo, Z., Liu, S., Li, W., WeiTang, Dong, H., 2016. Effects of deficit irrigation and plant density on the growth, yield and fiber quality of irrigated cotton. Field Crops Res. 197, 1–9. https://doi.org/10.1016/j.fcr.2016.06.003.

Zhang, H., Zhao, J., Hong, M., Ma, L., 2025. Optimization of deficit irrigation system for drip-irrigated corn in northern Xinjiang using dynamic reconstruction and dual physics-informed neural networks to drive AquaCrop. Front. Plant Sci. 16. https://doi.org/10.3389/fpls.2025.1678277.

Zhang, J., Guan, K., Peng, B., Pan, M., Zhou, W., Jiang, C., Kimm, H., Franz, T.E., Grant, R.F., Yang, Y., Rudnick, D.R., Heeren, D.M., Suyker, A.E., Bauerle, W.L., Miner, G.L., 2021. Sustainable irrigation based on co-regulation of soil water supply and atmospheric evaporative demand. Nat. Commun. 12, 5549. https://doi.org/10.1038/s41467-021-25254-7.

Zhao, J., 2022. Effects Ofadding Bio-organie Fertilizer for Drip Lrrigation Under'film Mulch on Cotton Yield. Nutr. Uptake Soil Salin.

Zhou, H., Chen, J., Ding, X., Qin, Q., Han, L., 2025. Future climate change will strengthen cotton production but have substantial environmental costs - A focus on Xinjiang by APSIM modelling. J. Clean. Prod. 491, 144803. https://doi.org/10.1016/j.jclepro.2025.144803.

Zhu, H., Zheng, B., Nie, W., Fei, L., Shan, Y., Li, G., Liang, F., 2024. Optimization of maize irrigation strategy in Xinjiang, China by AquaCrop based on a four-year study. Agric. Water Manag. 297, 108816. https://doi.org/10.1016/j.agwat.2024.108816.